Title
Microfluidic Generation of Viscoelastic Artificial Antigen Presenting Cells for T cell Activation

Author
Zhu, Yu

Publication Date
2022

Peer reviewed|Thesis/dissertation

UNIVERSITY OF CALIFORNIA
Los Angeles

Microfluidic Generation of Viscoelastic Artificial Antigen Presenting Cells for T cell Activation

A thesis submitted in partial satisfaction of

the requirements for the degree Master of Science

in Bioengineering

by

Yu Zhu

2022

ABSTRACT OF THE THESIS

Microfluidic Generation of Viscoelastic Artificial

Antigen Presenting Cells for T cell Activation

by

Yu Zhu

Master of Science in Bioengineering

University of California, Los Angeles, 2022

Professor Song Li, Chair

Artificial antigen presenting cells (aAPCs) are engineered platforms for T-cell activation. It has been widely used for the ex vivo generation of tumor-reactive lymphocytes to ample numbers for effective Adopted Cell Transfer (ACT) therapies including Chimeric Antigen Receptor (CAR) T cell therapy.

Viscoelastic materials with stress relaxation are closer to living tissues than pure elastic materials, which can be used to tune cell spreading, proliferation, or differentiation. By controlling molecular weight in combination with crosslinker concentration, we can adjust the stress relaxation properties of materials and therefore modulate cell behavior that is cocultured with viscoelastic biomaterials. It has also been found that T cells could sense the mechanical properties of the substrate and show different morphology when cultured on the substrate with different stiffness.

Based on the modulation of cell behavior by viscoelastic materials as well as the mechanosensing properties of T cells, a hypothesis could be made that viscoelastic materials may help improve T cell expansion and generate more proliferative T cell subgroups. There are already publications about the cell response to the matrix with different viscoelasticity using alginate hydrogel modified with adhesion molecules. However, no study has been conducted to investigate the T cell response to the viscoelastic properties of aAPCs. This is due to several technical issues including the fabrication of homogeneous, cell-sized alginate microgel, as well as the conjugation of T cell- specific antibodies to the microgel.

In this study, we overcame some of the technical issues and successfully fabricated viscoelastic aAPCs using ionically-crosslinked alginate, which can be applied to in vitro T cell activation and expansion. The alginate microbeads are generated using a microfluidic platform and then conjugated with T-cell-specific antibodies by click chemistry. These viscoelastic aAPCs show homogenous size distribution, low cytotoxicity and can be easily dissolved and removed after coculture. The T cell activation rate of these aAPCs is close to widely-used commercial aAPCs like Dynabeads. Therefore, this kind of viscoelastic aAPCs can serve as the platform to study how viscoelastic properties could affect T cell stimulation, and possess the potential to improve the quality of in vitro expanded T cells.

The thesis of Yu Zhu is approved.

Jun Chen

Timothy J. Deming

Song Li, Committee Chair

University of California, Los Angeles

2022

Table of Contents

List of Figures

Acknowledgments

I would like to thank my advisor, Prof. Song Li, for his kind instruction during my master's study. As the chair of the department of Bioengineering, he still spends enough time with every student in the lab and gives constructive and practical advice for the projects. I may not have the current critical thinking and scientific skills without his guidance.

I would thank Dr. Zeyang Liu for his instruction in my project. I enjoyed working with him throughout the whole time. He did not mind my mistakes in some experiments and gave precise advice on experimental design and troubleshooting sessions, which is very helpful in the formation of my experimental habit. I learned a lot of lab skills and developed strong insight and keen observation during the process.

I would also give special thanks to Dr. Jun Chen and Dr. Timothy J. Deming to serve on my master's thesis committee. Thank you for the advice on academic writing and revision of the thesis.

I would like to thank people in Dr. Song Li's lab, including Jennifer Soto for daily task management; Yang Song and Andy Chen for the microfluidic device fabrication; Tyler Hoffman and Yifan Wu for hydrogel preparation and characterization; Mahdi Hasani for T cell study; Jana Zarubova for cell culture; Xiao Han for antibody conjugation; Youcheng Yang for troubleshooting in the click chemistry experiment. I learned many things from different people, which finally makes me who I am.

I greatly thank my parents, Ying Yang & Kangsheng Zhu for their support during my study overseas. It is their encouragement and support that make me determined to pursue this master's degree. I would never have the current achievement without my parent's love.

Finally, to all of the people who have sacrificed their time for this creative work.

Chapter 1　Introduction to artificial antigen presenting cells (aAPCs)

1.1 Manufacture and expansion of CAR T cells

CAR T therapy is a newly emerged kind of cancer therapy in recent years. Briefly, in CAR T immunotherapy, T cells are modified with a special kind of reporter protein called chimeric antigen receptor that can target antigens antigen. [1] Genetically modified T cells are then infused back into patients to target attack and kill the cancer cells.

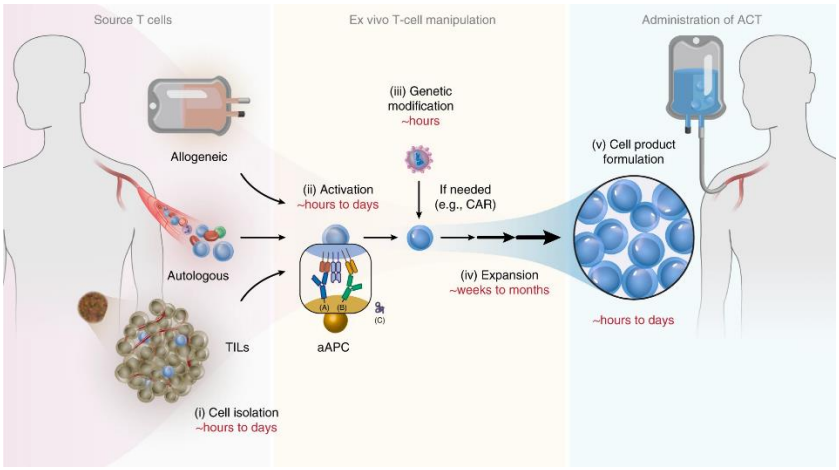

Figure 1-1 Schematic illustration of the production of therapeutic CAR T cells.
The process includes: 1) cell isolation, 2) T-cell activation, 3) genetic modification (if necessary), 4) T-cell expansion, and 5) cell product formulation. [2]

CAR T cells can be both CD4 and CD8 T cells, and infusion of both CAR T cells can provide synergic antitumor efficacy.[2] Some studies suggest that in solid tumor models, $CD4^+$ CAR T cells are indeed superior over $CD8^+$ T cells since they are less sensitive toward exhaustion. But currently, CAR-T cells may not be able to penetrate tumor tissue through the vascular endothelium. The clinically approved CAR-T therapies were only applied to hematological tumors, as CAR-T cells could return to the bloodstream and lymphatic system and have more contact with blood tumor cells.[3] Therefore, most research on CAR T cell

fabrication focus on the activity of CD8 T cells. It is generally believed that the efficacy of adoptive cell therapy is mostly attributed to CD8 T cells[4], and infusion of CD8 CAR T cells alone was sufficient for treating B cell melanoma. T cells that are used to produce therapeutic CAR T cells can be autologous, allogeneic T cells, or tumor-infiltrating lymphocytes (TILs). [5]

1.2 Clinical CAR T production technologies

Early outcomes of many clinical phase I and II studies come from Kymriah of Novartis and Yescarta of KITE Pharma. And these two were also the earliest CAR T cell products approved by FDA.

Basically, peripheral blood from the patient is washed to remove anti-coagulants added during leukapheresis. Soluble monoclonal antibodies, coated magnetic beads, or artificial antigen presenting cells are then frequently used for activation. The CAR transgene is then delivered into the cell by lentiviral, retroviral, or non-viral methods such as transposon/transposase systems. The cells are then expanded in static or dynamic culture vessels or devices until they reach the required cell numbers. Finally, the media composition is adjusted according to the formulation and then the product is transferred to a suitable container for delivery or freezing.

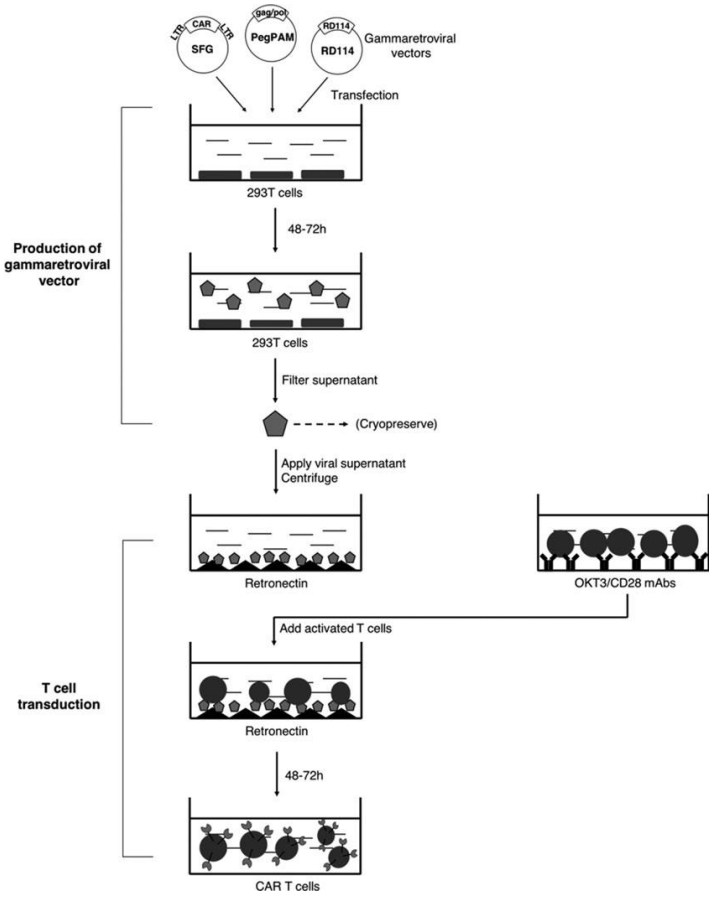

Figure 1-2 Flow chart of Clinical CAR T cell fabrication. 293T cells are transfected to produce gammaretroviral particles in culture media. The viral vector-containing supernatant is filtered and used to infect T cells previously activated by OKT3/CD28 monoclonal antibodies (mAbs). Upon viral entry into T cells, the CAR transgene is integrated into the cell genome to ensure stable long-term expression. [6]

However, research and development have still not established a mature, well-understood process for CAR T production. A number of CAR T products are manufactured using manual processing, which is labor intensive and difficult to scale, together with the prone to high failure rates.[7] This is mainly due to the requirement of personalized CAR T production as well as the lack of small-scale production technologies tailored for cell therapy. Production processes consistently comprise the same common steps shown in figure 1.1[8]. Therefore, a standard procedure for CAR T cell production is necessary for increasing the therapeutic effect of ACT therapies.

1.3 In vitro T cell expansion by artificial antigen presenting cells (aAPCs)

CAR T manufacture usually takes 10 days to 3 weeks to get enough cells for one treatment. Clinical adoptive T-cell therapy studies have shown that many CAR T cells are preferable, usually with up to 10^{11} T-cells infused into the patient. Therefore, the in vitro expansion and activation of T cells become a research focus to improve the quality of reinfused genetically-modified cells.[9]

Naturally, the endogenous T-cell activation is mediated by antigen presenting cells(APCs) such as dendritic cells (DCs) or macrophages. These cells process and present antigens on MHC molecules for recognition by certain lymphocytes like T cells. But coculturing T cells with DCs is a cumbersome process, due to the inherent variability of DCs and the logistics of maintaining separate culture systems.[10] Therefore, simplified activation strategies have been developed to avoid the usage of natural APCs for in vitro T cell activation. Some early studies used OKT3, IL-2, and irradiated peripheral blood mononuclear cell feeders for T cell activation. [11] But excessive cytokines and antigens can lead to an exhausted T cell product, displaying poor effector function and quickly approaching apoptosis.[12] Therefore, people have spurred interest in the usage of artificial antigen presenting cells (aAPCs) to provide greater control over T cell signaling and generate optimally effective CAR T cells for adoptive cell transfer therapy.[13]

1.4 Development of aAPCs

The basic concept of aAPCs started from the initial observation that T cells could be

stimulated by the interaction between anti-CD3 antibody and TCR, as well as the costimulatory signal of αCD28 and CD28, without the involvement of antigen-presented MHC molecule. [14] This can be achieved by either using engineered cells or biomaterials-based beads to fabricate the desired aAPCs.

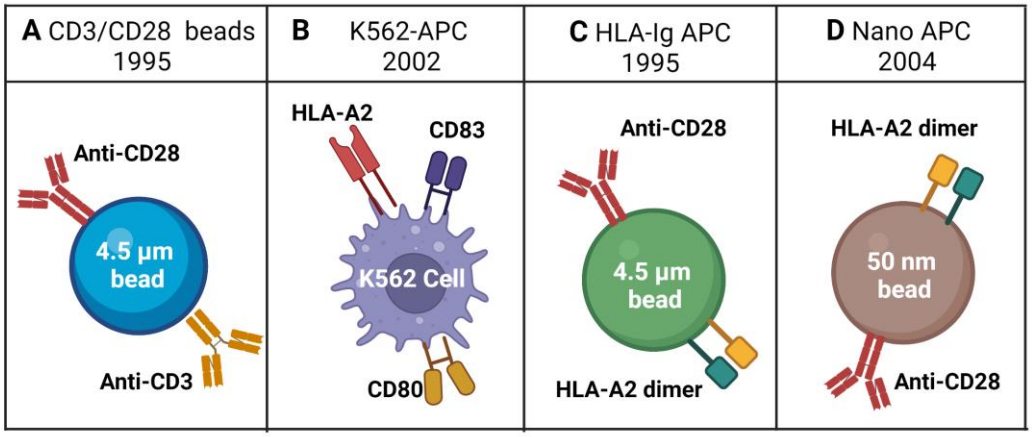

Figure 1-3 Artificial APC that has been developed for ACT.[15] A) Early stage anti-CD3/CD28 aAPCs B) K562-cell based aAPCs developed from a human myelogenous leukemia cell line C) HLA-Ig aAPCs that replace anti-CD3 HLA-antigen complex D) Nanoparticle-based aAPCs.

1.4.1 Cell-based aAPCs

The aAPCs system can be roughly classified as cell-based aAPCs and synthetic aAPCs. Cell-based aAPCs are derived from primary or transformed human or xenogeneic cells, which can be engineered using lentiviral transduction to express necessary TCR, costimulatory, or signals required for immune synapse formation.[13] And potential deleterious or negative regulatory signals can be deleted by genetic editing. The advantage of cell-based aAPCs is that once generated, the cell lines can be banked and kept as a long-term readily accessible source of reagent to use for T cell generation or expansion, without the need to

prepare autologous APC or feeder cells.[16] Originally, autologous aAPCs such as dendritic cells, monocytes, or activated B cells have been used to generate tumor-specific T cells. However, the requirement for cancer patients' blood to prepare autologous APC from each patient is time-consuming.

One of the most widely studied cell-based aAPCs is the K562 cell-based aAPCs. This is a kind of human erythroleukemia cell that does not express endogenous HLA molecules. They are not able to induce allogeneic T cell proliferation by themselves but do express ICAM-1 and LFA-3 that is required for forming immune synapse during in vivo T cell activation.[17] Therefore, by transducing the K562 cells with the anti-CD3 and anti-CD28 monoclonal antibodies, they become the qualified APCs that can induce the non-specific proliferation of T cells. K562 cells also secrete IL-15, which can help maintain the viability of $CD8^+$ T cells in long-term culture. One clinical grade K562 cell-based aAPC-A2 line called clone 33 was used to expand MART-1 specific T cells against advanced melanoma.[18] These K562-based aAPCs were transfected with four non-retroviral plasmids that encode for HLA- A2, CD80, CD83, and a puromycin resistance gene. Compared to the natural DC cells, aAPCs-A2 clone 33 could expand MART-1-specific T cells from both healthy donors and patients with metastatic melanoma (19–49% tetramer positive) in a similar way. [19]

However, K562 cells also express many negative regulatory molecules like PD-L1, or B7-H3, which makes the K562 based aAPCs a complicated activation system. [20] Another reason that the K562 aAPCs platform has not been widely used for cancer therapy, is the fact that these cells are derived from a malignant clone. Although K562 cell-based aAPCs are irradiated before co-culturing with T cells so that none of them are detected after T cell

expansions, there are appropriate probabilities in infusing T cell products with a malignant cell line into cancer patients. [15]

1.4.2 Lipid-based APCs

Synthetic aAPCs are generally microscale biomaterials anchored with anti-CD3 and anti-CD28 that can induce T cell proliferation independent of antigen stimulation. By immobilizing anti-CD3 and anti-CD28 on a plate to simultaneously deliver signal 1 and a costimulatory signal 2, T cell proliferation can be increased without provoking early cell death.[21] The expanded cells also demonstrate an enhanced ability to release cytokines and lyse target cells in an MHC unrestricted manner.[22]

Although robust proliferation could be achieved using a culture plate coated with αCD3 and αCD28, the interaction between T cell and culture dish can not mimic the natural immune synapse(IS), which makes it inferior to the aAPCs system. [13] Besides the antibody-coated plates, acellular APC systems also include bead-based aAPCs and ligand incorporated lipid vesicles.[23]

The importance of mobility of molecules that participate in an immune synapse between a natural APC and a T cell has been recognized as a critical component in efficient TCR signaling, and antigen presentation by exosomes, liposomes, and other lipid preparations might represent a means to recapitulate this in an artificial setting. Lipid vesicles have not yet been widely explored as aAPCs for in vitro T cell expansion. But since the formation of immune synapse requires the actin reorganization and recruitment of several other molecules to the TCR, the engineered lipid vesicles may have the potential to improve immune synapse

formation due to the mobility of the lipid surface and hence the flexibility for surface molecule movement.[24]

Exosomes are vesicles secreted from cellular endosomes that present antigens with HLA class I and II molecules, as well as provide costimulatory and adhesion signals for T cell activation. [25]Exosomes derived from dendritic cells could be used as an artificial acellular vaccine for murine mastocytoma and mammary carcinoma, and induced anti-tumor immune responses in vivo, despite relatively weak T cell stimulation in vitro.[25] Tumor-derived exosomes also appear to induce more efficient T cell stimulation in vivo than in vitro, suggesting that cross-priming by endogenous professional APCs might be required for optimal T cell stimulation. [26] However, the requirement for cross-priming to induce CD8+ T cell proliferation by tumor-derived exosomes also indicates that this approach may not be the optimal aAPCs preparation for in vitro expansion of T cells.[17]

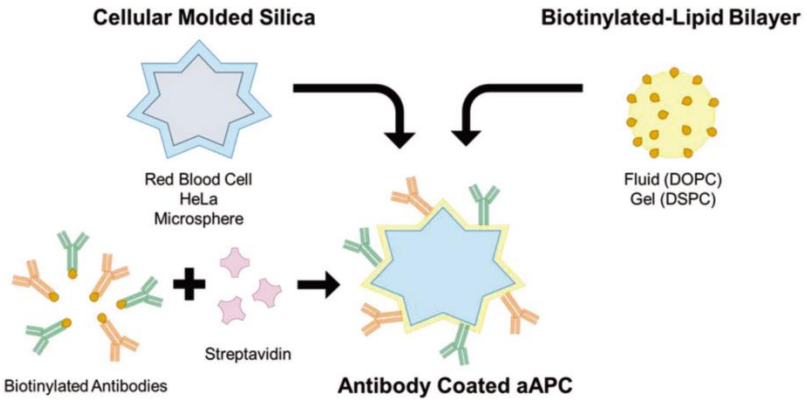

Figure 1-4 Schematic of the synthesis of silica microparticles with supported lipid bilayers.[27]

Besides using only lipid particles as aAPCs, microparticles with supported lipid bilayers seem to be a more reasonable choice to fabricate aAPCs. Olden et al. fabricated aAPCs using supported lipid bilayers on various cell-sized silica microparticles with defined

membrane fluidity and stimulating antibody density.[27] These aAPCs are able to stimulate T cell growth, and preferentially promote $CD8^+$ T cell growth over $CD4^+$ T cell growth compared to some commercially available antibody-conjugated particles. T cells activated using the lipid aAPCs show less-differentiated and less-exhausted phenotypes when cocultured with Hela cells

1.4.3 Synthetic aAPCs

Polystyrene beads-based aAPCs are one of the most popular aAPCs systems in recent years. Commercial products like Dynabeads magnetic beads have been widely used for T cell study.

Polystyrene beads can be manufactured under stable conditions that resulted in uniformity of size. Currently, the beads between 5-6 μm in diameter were found to be the optimal size for stimulation of T cells compared to those of smaller dimensions. Beads coated with anti-CD3 could deliver antigen-independent signals to polyclonal T cells in a format that is more closely approximate to an immune synapse than solid phase planar systems. Also, costimulatory or inhibitory signals can be provided by covalently binding agonistic or antagonistic ligands and/or antibodies to the beads(figure12). This approach has successfully been exploited in multiple studies to investigate the signals involved in the T cell response to TCR ligation and to expand T cells for in vitro and in vivo use in patients[28]

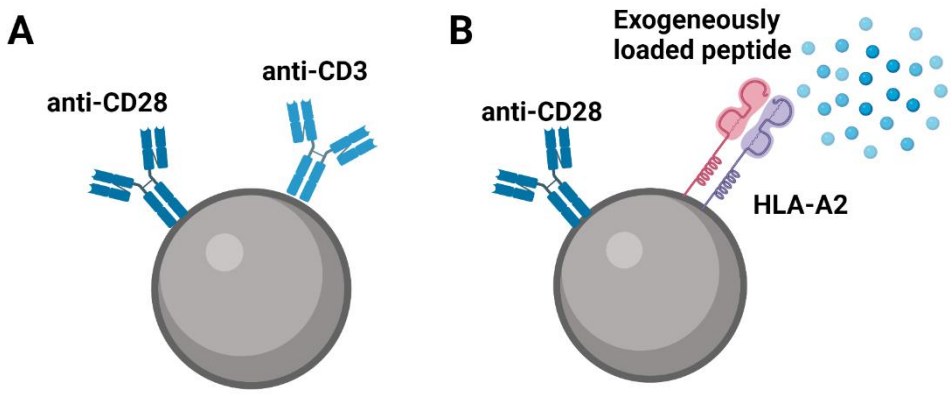

Figure 1-5 Polystyrene aAPCs conjugated with anti-CD 28 costimulatory molecule and A) Anti-CD3, B) Antigen-MHC complex.[13]

Beads-based aAPCs have been endowed with antigen specificity by coating the bead with MHC-peptide single chain construct dimers or tetramers. An improvement that bypassed the need to coat the beads with MHC-peptide complex is to bind dimeric HLA-A2-immunoglobulin fusion molecules to the beads, which can then be loaded exogenously with peptide antigen. This strategy was combined with bound αCD28 to provide co-stimulation and effectively expanded antigen-specific T cells ex vivo.[29]

Some clinical studies have used anti-CD3/anti-CD28 paramagnetic bead-based aAPCs to expand autologous T cells, which were then infused into patients with non-Hodgkin's lymphoma or Chronic Myeloid Leukemia (CML) after autologous $CD34^+$ selected hematopoietic stem cell transplantation (HSCT)[30, 31]. Due to the magnetic particles incorporated in the beads, the beads can be efficiently removed by magnetic depletion before infusion. Robust in vitro T cell expansion was also achieved. CD3+ T cells from an allogeneic stem cell transplant donor have also been expanded with anti-CD3/anti-CD28 beads and infused in doses of $1 \times 10^6 – 1 \times 10^8$ CD3+ cells/kg to post-transplant patients that

had relapsed with hematologic malignancies after allogeneic transplant[32]. The CD4:CD8 T cell ratio remained constant during the expansion and a mean of 113±26.3 fold expansion was achieved during a 12-day culture.

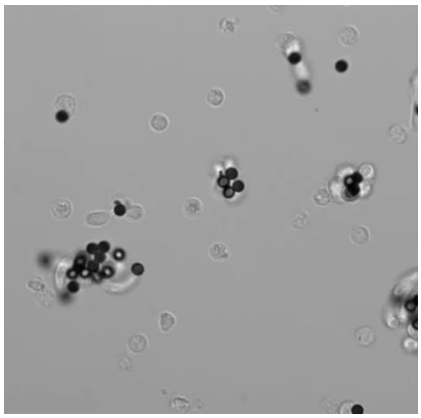

Figure 1-6 Image of T cell activation by Gibco magnetic polystyrene aAPCs.

When using polystyrene beads to activate T cells, cytokines have to be added to the culture, leading to high overall IL-2 dosage and fluctuation in IL-2 concentration. This could also increase the side effects due to co-injection of IL-2 during reinfusion of T cells into patients. [33] Implementation of mechanisms that allow continuous cytokine release by aAPCs may therefore further improve their potential to activate and differentiate T cells. In particular, cytokine release may be essential for the development of functional CD8+ T cells that can generate potent immune responses. Therefore, biodegradable poly(lactic-co-glycolic acid) (PLGA) microparticles can also serve as a good alternative to the current design of aAPCs. The PLGA particles are stable during the initial T cell activation and may degrade later and constantly release IL-2, which may be one important characteristic for future studies.

Limitations of beads-based aAPCs include that spherical beads are incapable of mimicking the dynamic remodeling of the cell membrane that is established at the immune synapse between professional APC and T cells. The expansion and viability of T cells can

also be a problem with beads-based culture systems. Early studies found that CD8+T cells expanded with αCD3/αCD28 beads less well than their $CD4^+$ counterparts, and the viability of $CD8^+$ T cells was poor after long periods of in vitro culture Also, the incorporation of additional signaling molecules on the beads requires purification of recombinant protein and linking the protein to the bead, which is often more difficult than transfecting cell-based aAPCs. [29]

Chapter 2 Application of alginate hydrogel in biological study

2.1 Chemical structure of alginate

Alginate is a negatively charged biopolymer that is originally isolated from brown seaweeds and has been extensively investigated and used for many biomedical applications, due to its biocompatibility, low cytotoxicity, and relatively low cost. [34]Alginate gels can also be loaded with drug molecules, from small chemical drugs to macromolecular proteins, and released in a controlled manner, depending on the cross-linker types and cross-linking methods.

The structural similarity to extracellular matrices of living tissues makes alginate a good carrier for bioactive agents such as small chemical drugs and proteins.

Alginate hydrogels can be prepared by various cross-linking methods, and their structural similarity to extracellular matrices (ECM) of living tissues allows wide applications in wound healing, delivery of bioactive agents such as small chemical drugs and proteins, and cell transplantation. Alginate is now known to be a kind of linear copolymer containing blocks of (1,4)-linked β-d-mannuronate (M) and α-l-guluronate (G) residues. The blocks are composed of consecutive G residues, consecutive M residues, or alternating M and G residues. Alginates extracted from different sources differ in M and G contents as well as the length of each block, and more than 200 types of different alginates are currently being manufactured. [35] However, only the G-blocks of alginate are able to participate in intermolecular cross-linking with divalent cations (Ca^{2+}, $Cu^{2+)}$ to form hydrogels, due to that G-blocks are bent or distorted while M-blocks extended ribbon-like form.[36]

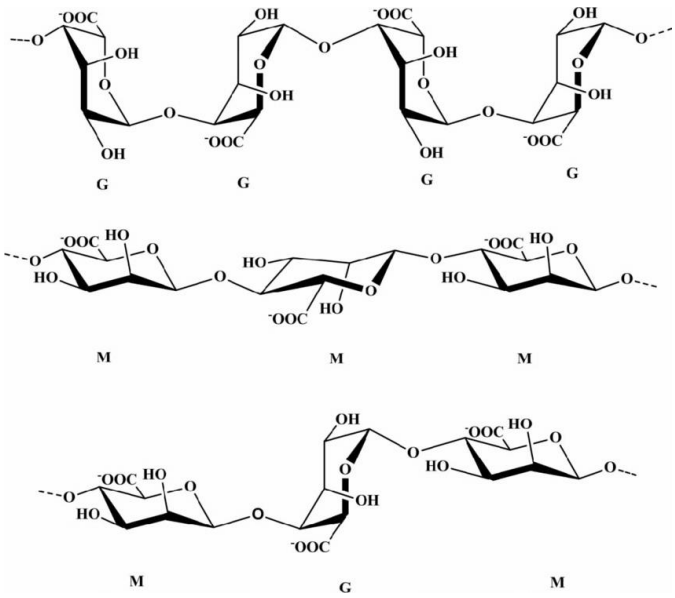

Figure 2-1 Chemical structure of alginate polymer chain. There are G-block, M-block, or alternating G and M-blocks in alginate. [37]

The composition (i.e., M/G ratio), G-block length, and molecular weight are therefore critical factors for the physical properties of alginate and thus the hydrogels.[38] The mechanical properties of alginate gels can be adjusted by increasing the length of the G-block and molecular weight. Besides the composition of the polymer chain, pH may also affect the mechanical property of alginate. The viscosity of alginate solutions may increase as pH decreases, and reach a maximum at around pH 3–3.5. This is because carboxylate groups in the alginate backbone become protonated and form hydrogen bonds.[39]

2.2 Gelation of alginate

Alginate is typically used in the form of hydrogel in biomedical applications, including wound healing, drug delivery, and tissue engineering. Hydrogels are three-dimensional cross-linked networks that hold a large amount of water while maintaining the structure due to chemical or physical cross-linking of polymer chains. They are often biocompatible, as they

are structurally similar to the macromolecular-based components in the body, and can often be delivered into the body via minimally invasive administration.[40] Chemical and/or physical cross-linking of hydrophilic polymers are typical approaches to forming hydrogels, and their physicochemical properties are highly dependent on the cross-linking type and cross-linking density, in addition to the molecular weight and chemical composition of the polymers.[41]

2.2.1 Ionically crosslinked hydrogel

The most common method to prepare hydrogels from an alginate solution is adding ionic cross-linking agents, such as divalent cations (i.e., Ca^{2+}). The divalent cations are believed to bind solely to G blocks of the alginate chains, as the flexibility of the G blocks allows a high degree of coordination between the divalent ions and carboxylic groups. The G blocks of one polymer then form junctions with the G blocks of adjacent polymer chains in what is termed the egg-box model of cross-linking, resulting in a gel structure.[42]

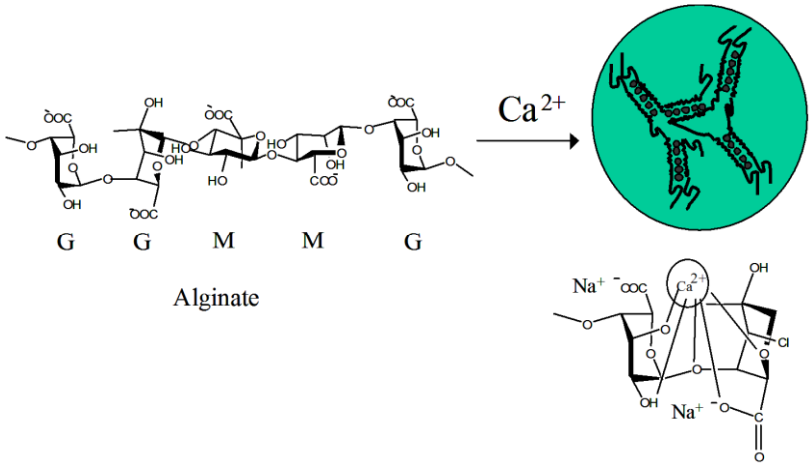

Figure 2-2 Mechanism of alginate ionic gelation.[43]

Calcium chloride ($CaCl_2$) is one of the most frequently used agents to ionically cross-link

alginate. However, the chelation process is too fast that it leads to poorly controlled gelation, especially at high concentrations. One approach to slow and control gelation is to utilize a buffer containing phosphate (e.g. PBS buffer), as phosphate groups in the buffer compete with carboxylate groups of alginate in the reaction with calcium ions, and retard the reaction. Calcium sulfate ($CaSO_4$) and calcium carbonate ($CaCO_3$), due to their lower solubilities, can also slow down the gelation rate and widen the working time for alginate gels. As the low amount of dissolved Ca^{2+} is used for gelation, the undissolved $CaSO_4$ will dissociate and release more Ca^{2+} that subsequently initiates the gelation of the alginate solution in a more gradual manner .[44] Ethylenediaminetetraacetic Acid (EDTA) chelated with Calcium ion (Ca-EDTA) is also served as a good alternative. Through external stimulation by an acidic environment, Ca^{2+} can be released from the complex and cause the gelation of alginate.

2.2.2 Covalently crosslinked alginate

Covalent cross-linking of alginate with poly(ethylene glycol)-diamines of various molecular weights were first investigated in order to prepare gels with adjustable stiffness, as the elastic modulus can be adjusted by changing the cross-linking density or weight fraction of poly(ethylene glycol) (PEG) in the gel.

Compared to ionically crosslinked hydrogel, covalent alginate hydrogel does not have plastic deformation. Covalent cross-linking of alginate with poly(ethylene glycol)-diamines of various molecular weights were first investigated to prepare hydrogels with a wide range of mechanical properties. The elastic modulus of alginate could be adjusted by changing the

cross-linking density or weight fraction of poly(ethylene glycol) (PEG) in the gel. [45]Later some multi-functional molecules with hydrazides(e.g., poly(acrylamide-co-hydrazide)(PAH) and adipic acid dihydrazide(AAD)) are being developed as a crosslinker for alginate through the formation of hydrazone bonds between aldehydes and hydrazides. [46]

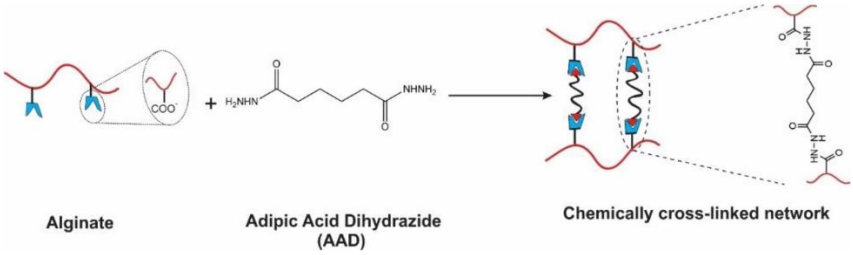

Figure 2-3 Mechanism of alginate covalent crosslinking by AAD, a diamine crosslinker. [36]

2.2.3 Photo crosslinking of alginate

Photo cross-linking is an interesting method that uses a photosensitive crosslinker to achieve in vivo gelation. Photo cross-linking can be carried out in mild reaction conditions, even in direct contact with drugs and cells, with the appropriate chemical initiators. Alginate, modified with 2-aminoethyl methacrylate and crosslinked by exposure to a laser at a specific wavelength in the presence of 0.05% photoinitiator, can form clear and flexible hydrogels. This rapid and controllable polymerization by an optical trigger allows for controlled in situ photopolymerizations in a minimally invasive manner. [47] But the potential cytotoxicity of the photoinitiator could be harmful to the body. Another method could be using PEG–anthracene grafted alginate. Anthracene dimerizes with other anthracene molecules upon exposure to 365 nm light and de-dimerizes with 254/248-nm light treatment in a reversible reaction, without releasing any harmful byproducts.

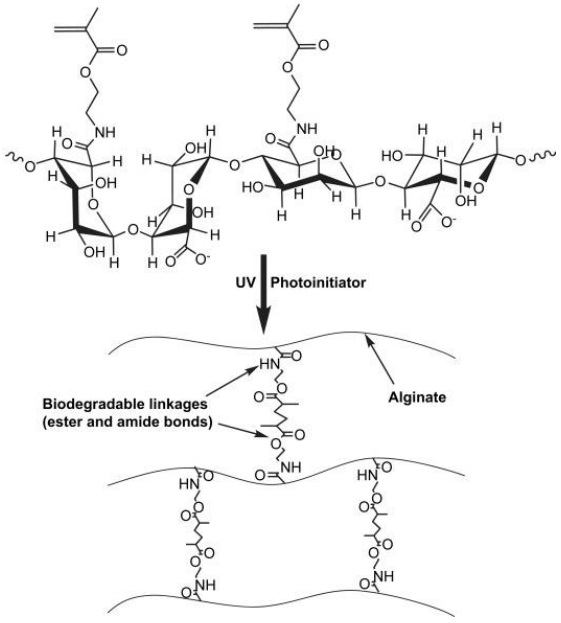

Figure 2-4 Alginate–anthracene with photo-reversible dimerization property.[47]

2.3 Viscoelastic alginate hydrogel for biological study

Alginate hydrogels have been used for many of the seminal studies on the impact of substrate viscoelasticity. One unique property of alginate is that the viscoelasticity of alginate hydrogel can be adjusted independently from other mechanical properties. Divalent cations like Ca^{2+} can bridge two G blocks to form an ionic crosslink between different alginate chains and lead to the gelation of a three-dimensional polymer network.[48] These weak ionic crosslinks can break under stress and then reform, allowing local matrix flow to dissipate stress and resulting in macroscopic stress relaxation of the hydrogel under an applied load.[49] The length of the G blocks is expected to control the length of the ionic crosslink zone, with the number of calcium ions packed between G-blocks controlling the strength of the bond, based on the "egg-box" model that described how cations are packed and be coordinated between the Polysaccharides.[50] Once the G-blocks are lined up with some minimum level of crosslinking, additional crosslinks fill in these crosslink junctions and cause no change to the

pore structure. As a result, the pore size of ionically crosslinked alginate hydrogels is not altered by increased crosslinking, as has been established by diffusion studies.[51]

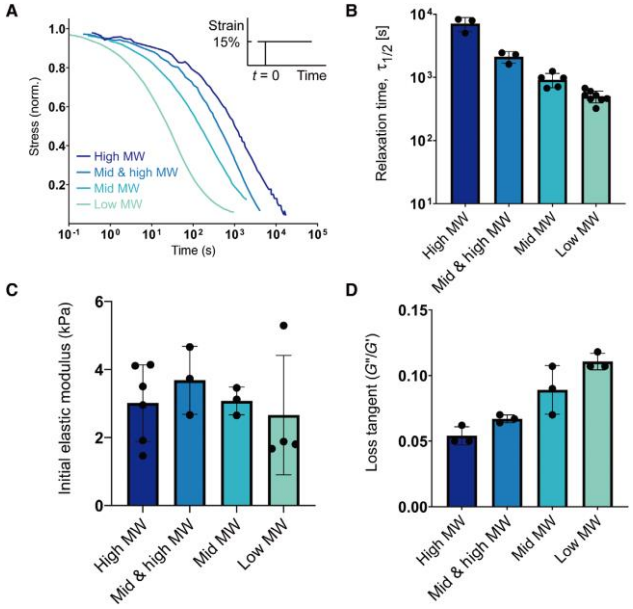

Figure 2-5 Ionically crosslinked hydrogels with similar stiffness but different relaxation time.
A) Stress relaxation profiles for hydrogels with varying alginate molecular weight. B) The characteristic timescale of stress relaxation for the different alginate hydrogels. For y axis, $\tau_{1/2}$ is the relaxation time defined by the timescale at which the stress is relaxed to half its original value. C) Initial elastic modulus (stiffness) for the different alginate hydrogels. D) Loss tangent (ratio of loss modulus to storage modulus) for the different alginate hydrogels. [52]

Viscoelasticity in alginate hydrogels can be tuned by varying the molecular weight of the alginate polymer, changing the type of crosslinker (ionic vs covalent), or by grafting short poly(ethylene-glycol) (PEG) chains to the alginate polymer. The simplest method would be using different molecular weight polymers in combination with different crosslinking densities of calcium. The stress relaxation properties of the resulting hydrogels could be modulated owing to the altered connectivity and chain mobility in the network. [53] In other words, the relaxation time can be extended by lowering the average molecular weight (MW) of alginate, while the loss of stiffness caused by lower MW can be compensated by adding an

extra amount of crosslinker. Therefore, different alginate hydrogels with similar stiffness but different relaxation time can be fabricated to study the effect of viscoelasticity on cell behavior. Then covalently crosslinked alginate with similar stiffness can be made to study the cell behavior on viscoelastic material versus pure elastic surface. Generally, alginate is mixed with EDC, which creates crosslinks between carboxyl groups and primary amines. Because alginate does not contain amine groups, a diamine such as adipic acid dihydrazide (AAD) is added to link carboxyl groups on different alginate chains.

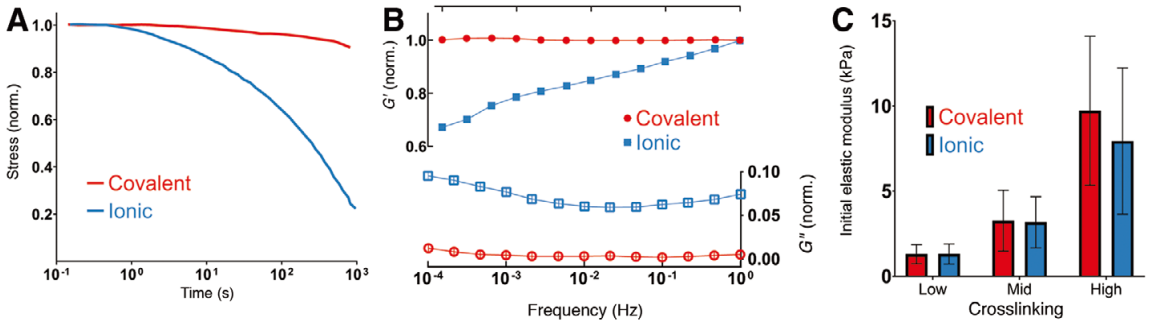

Figure 2-6 Mechanical properties of ionically versus covalently crosslinked alginate hydrogels. A) Stress relaxation profiles for covalently versus ionically crosslinked alginate hydrogels. B) Storage modulus (G′) and loss modulus (G”) as a function of frequency for ionically versus covalently crosslinked alginate hydrogels. C) Initial elastic modulus (stiffness) for covalently versus ionically crosslinked alginate hydrogels. The concentration of crosslinker is adjusted to generate hydrogel with similar stiffness for low, medium, and high stiffness groups relatively.[52]

Another method to adjust viscoelasticity would be using commercially available PEG-amines of varying molecular weights, which can be covalently coupled to the alginate polymer backbone at varying concentrations with simple carbodiimide chemistry. This is because the covalent coupling of short PEG spacers to the alginate would provide a steric hindrance to crosslinking of alginate chains and therefore enhance stress relaxation in the gel. The stress relaxation of alginate-PEG hydrogels is determined by the total mass amount of

added PEG rather than the molecular weight or concentration of PEG alone, with more PEG leading to faster stress relaxation, enhanced creep, and a higher loss modulus.[54] This approach enables precise tuning of stress relaxation over a wide range while using the same molecular weight of commercially available alginate. A key advantage of this approach is that the addition of PEG to the alginate leads to hydrogels with faster stress relaxation and a higher loss modulus, extending the range of accessible stress relaxation times relative to alginate-only hydrogels.[55] One limitation is that varying the PEG amount will likely affect the pore size of the alginate hydrogel. In addition, it is possible that adding large amounts of PEG could limit the availability of sites to conjugate RGD or other adhesion ligands and that RGD ligands close to PEG chains could be less accessible to cells for adhesion.

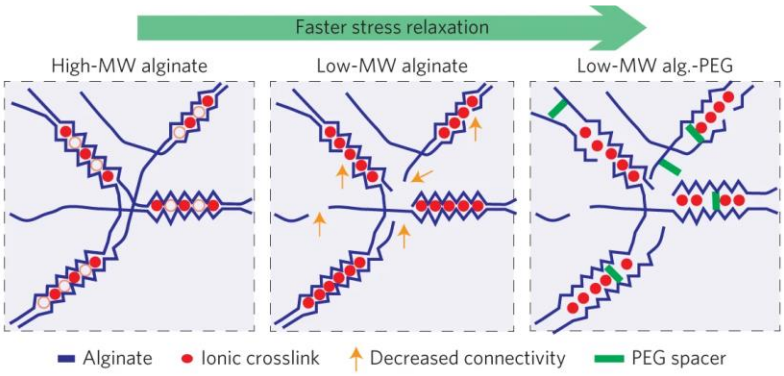

Figure 2-7 Schematic depicting how lowering the molecular weight (MW) of alginate polymers (blue) crosslinked by calcium (red) decreases entanglement and connectivity (orange arrows) of the network, and coupling of small spacers provides a steric spacing of crosslinking zones in the alginate.[55]

Chapter 3 Microfluidic fabrication of microparticles for biomedical applications

3.1 Fabrication of microparticles by microfluidic devices

Droplet-based microfluidics can manipulate discrete volumes of fluids in immiscible phases while maintaining low Reynolds number and laminar flow regimes in the system.[56] Droplet microfluidics can offer accurate control over the flows of multiple fluids on the microscale, enabling the fabrication of different microparticles with precisely tunable structures and compositions in a high throughput manner. The combination of these outstanding features of droplet-based microfluidics, together with proper materials and fabrication methods, can achieve highly effective production of microparticles whose features and functionalities can be well controlled. These microparticles have great potential in a wide range of biomedical applications including drug delivery, cell-laden matrices, biosensors, and serving as artificial cells. [57]

These applications of microparticles depend on their properties, which are affected by their size, structure, composition, and configuration. Therefore, it is essential to fabricate microparticles in a controlled manner to improve their pharmaceutical capability and reliability for biological studies.[58, 59] However, it is pretty challenging to produce microparticles with expected properties through conventional methods including emulsion polymerization, dispersion polymerization, and spray drying. [60] These methods usually result in microparticles with large polydispersity, poor reproducibility, and uneven morphology, even within one experiment. To overcome these limitations, various technologies, including droplet microfluidics, photolithography, flow lithography microfluidics, soft lithography-

based imprinting, and micro-molding have been explored for generating microparticles more controllable with more stable properties.[61] Among these, droplet microfluidics is one of the most effective techniques for microparticle fabrication. It offers accurate control over multiple fluids at the microscale within one device, which allows precise tuning of the compositions and geometrical characteristics of microparticles.[62] Exploiting these advantages, engineered microparticles with controlled sizes, monodispersity, diverse morphologies, and specific functions can be generated, and are playing an increasingly important role in biomedical fields.[63] For instance, as drug delivery vehicles, microcapsules or microparticles with core-shell structure can be prepared with well-defined structures and compositions that allow for high drug encapsulation efficiency and well-controlled release of the encapsulants.[59, 64] As cell carriers, hydrogel microparticles can be produced to act as extracellular matrix (ECM) to provide a better environment for cell growth and maintain efficient nutrient and metabolic exchanges for long term cell culture.[65] In addition, liposomes or polymersomes with multicompartment structures can be generated by droplet microfluidics. Their mechanical properties can be adjusted to the same level as natural cells, making them ideal candidates for artificial cells. [66]

3.2 Introduction to droplet-based microfluidics

3.2.1 Mechanism of droplet generation

The droplets generated in droplet-based microfluidics can serve as microreactors to carry out physical, chemical, or biological reactions. Due to the small channel size(nL to μL

volume), they require only a small quantity of reactants each time. The principle of droplet-based microfluidics is similar to that of conventional emulsification, which consists of mixing two immiscible liquids. But the emulsion in a microfluidic device can be produced by precisely fabricating one drop at a time. This process is an outcome of a well-controlled balance between various forces acting on the fluid flow.[67] There are various modes of droplet breakup at the outlet including squeezing, dripping, jetting, tip-streaming, and tip-multi-breaking. Among them, the dripping mode is most widely utilized due to the high monodispersity of the droplets generated.[67] The droplet breakup modes can be applied to various channel geometries including cross-flow, co-flow, and flow-focusing.

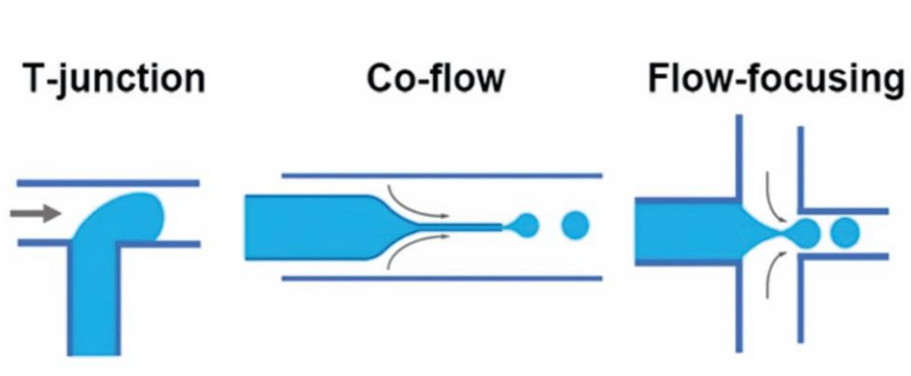

Figure 3-1 Schematic illustration of microparticle generation in the flow-focusing microfluidic device.

The T-junction (cross-flow) geometry is widely used in the production of single emulsions due to the simplicity of device fabrication, which requires no additional alignment. The droplets generated have high monodispersity, and the size of the droplets generated in a T-junction is generally larger than 10 μm due to the limitation of the channel dimension. In the co-flow geometry, the dispersed phase channel is inserted into the continuous phase channel and forms a coaxial structure. The droplet sizes are larger than the tip diameter, thus,

are typically larger than 10 μm. The flow-focusing mode has a structure that suddenly shrinks the fluid passageway. Fluid phases form a hydrodynamic flow that contracts through the focus unit resulting in high fluid flow rate. This enhances the viscous shear force and allows the formation of droplets with sizes down to a few hundred nanometers.

3.2.2 Capillary & PDMS microfluidic devices

Fabrication of microfluidic devices with well-defined geometry and material compatibility is important for generating and manipulating droplets. Two main types of droplet microfluidic devices are used in generating various types of emulsion droplets. One is glass capillary microfluidics which has the advantage of high chemical resistance and ideal coaxial flow-focusing which enables the preparation of droplets with a wide range of material compositions and structures. The other is lithographically fabricated poly(dimethylsiloxane) (PDMS) devices that have the advantage of preparing a large number of identical devices, making them attractive for large-scale production of the droplet.[67]

One advantage of capillary microfluidic devices is that they do not require a complicated fabrication process and are simple and highly robust. Also, they only involve simply assembling basic modules including injection tubes, transition tubes, and collection tubes.[68] Typically, a capillary microfluidic device consists of coaxial assemblies of glass capillaries. For example, a tapered cylindrical glass capillary is carefully inserted into a square glass capillary to form water-in-oil (W/O) or oil-in-water (O/W) single emulsion droplets.

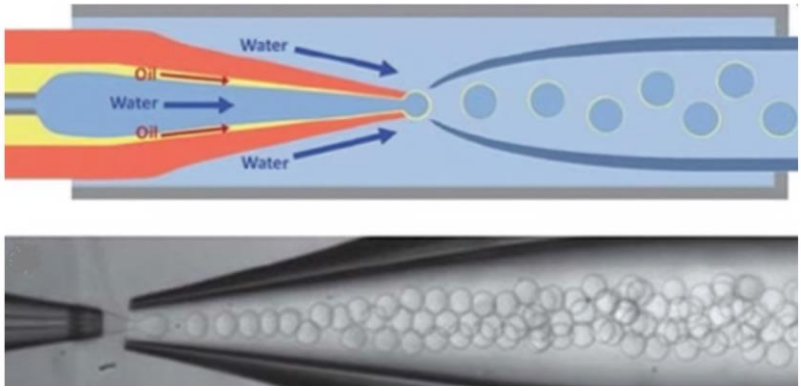

Figure 3-2 Schematic illustration of the capillary microfluidic devices for preparation of droplets.[69]

Prior to insertion, the injection cylindrical capillary surface is rendered to have a higher affinity to the continuous phase than to the dispersed phase; this prevents the adhesion or wetting of droplets on the capillary surface. The surface is rendered hydrophobic for W/O single emulsion, whereas it is rendered hydrophilic for O/W single emulsion.

While capillary microfluidic devices are easy to assemble and feature high precision flow control, the manual fabrication process makes it difficult to prepare more than a few devices at a time and the devices prepared often suffer from a lack of reproducibility. Thus, PDMS devices can serve as a good alternative, due to the simple and reproducible device fabrication procedures. Such PDMS devices are prepared using soft lithography which enables the formation of identical devices through duplicated molding, fabrication of devices with micron-scale resolution, and greater flexibility in the channel design compared to capillary devices. Moreover, PDMS is optically transparent, biologically inert, permeable to gases, and low in cost of fabrication, which makes it a more cost-effective option when a large quantity of microfluidic devices are needed.[70]

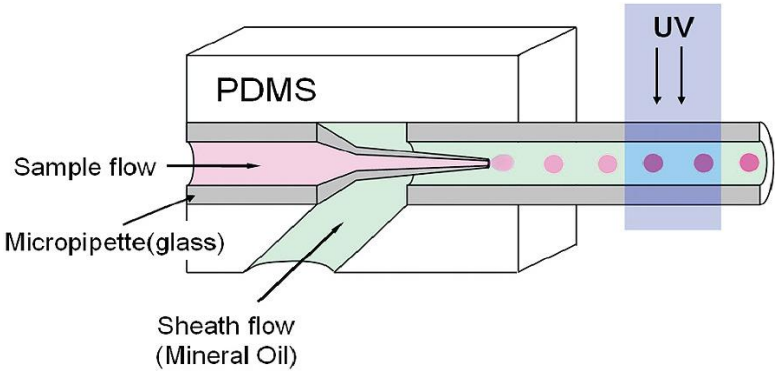

Figure 3-3 Schematic illustration of microfluidic generation of microparticles using PDMS device.[71]

Briefly, to fabricate three-dimensional microfluidic devices, the photomasks are first prepared. To create a device from the photomask, a silicon wafer is coated with a photoresist to the desired height of the microfluidic channels. The coated wafer is then heated to evaporate the solvent and cooled to solidify the coating. Then, the photomask is placed on top of the coated wafer and the two are exposed to ultra-violet (UV) light. The light that passes through the transparent regions of the photomask is crosslinked while the uncrosslinked parts are removed by using a solvent. To mold a microfluidic device from this "master," another polymer, PDMS is poured to form a clear, rubbery layer. Then, the imprinted side is bonded to either another block of PDMS or a glass substrate for sealing with an oxygen plasma treatment. Due to the high accuracy of photolithography technologies, the channel of PDMS microfluidic device could be several micrometers in diameter, which allows precise control of the flow.

While the PDMS device can be easily fabricated in mass production, the hydrophobic nature may limit the formation of emulsion droplets. For example, to form O/W single emulsions, the microchannel surface needs to be modified to be hydrophilic to ensure an effective wetting of the channel surface by the continuous aqueous phase.

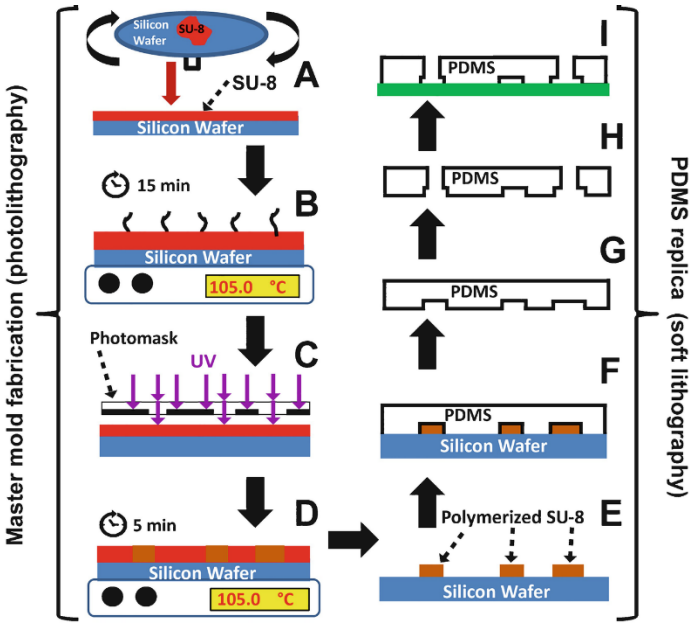

Figure 3-4 Flow chart of the PDMS microfluidic device fabrication A) Spin coat photoresist. B) Soft bake. C) Exposing photoresist through photomask. D) Postexposure bake. E) Development to obtain master mold. F) Pour PDMS over the master mold and cure. G) Peel off the cured PDMS slab. H) Punch tubing inlets in the PDMS replica. I) Seal the PDMS replica to a glass slide. [72]

3.3 Fabrication of alginate microparticles

Many mechanisms are involved in the fabrication of different microparticles, including polymerization, ionic crosslinking, and solvent evaporation. Since this study focus on the alginate microparticles, only alginate gelation is introduced in this part.

There are two methods for alginate gelation in the device, internal gelation, and external gelation. As for internal gelation, the cross-linkers are inside the alginate droplet. While in external gelation, the cross-linkers are mixed after the alginate particles form. Due to the slow gelation of covalent alginate, only ionic crosslinked alginate is used for the microparticles.

3.3.1 Internal gelation

Crosslinkers come from inside the alginate droplets and can be either soluble or

insoluble/slightly soluble in water. Water-soluble cross-linkers are usually divalent metal ions like barium chloride ($BaCl_2$) and calcium chloride ($CaCl_2$), and alginate is crosslinked directly at the interior of droplets. These agents can be mixed with Na-alginate before or after droplet generation.

As Zhang et al. did, using a 5-channel microfluidic device, sodium alginate fluid was mixed with mineral oil fluids with a surfactant (Span 80). Droplets were generated by co-flow. However, instead of producing discrete droplets, a line of knots connected with each other, which also caused the clogging of the channel. This phenomenon persisted even when different flow rates were used, due to the increased viscosity of mineral oil when alginate and $CaCl_2$ were mixed. [73] Theis problem can be solved using low viscosity oil and reducing the rate of gelation. A less concentrated Na-alginate solution, or a higher flow rate ratio between the continuous fluid and the dispersed fluid, may also help.

To fix these issues, Utech et al. presented another method for the fabrication of monodisperse alginate microgels with structural homogeneity through externally triggered crosslinking. They delivered calcium ions in the form of water-soluble calcium–ethylenediaminetetraacetic acid (calcium–EDTA) complex. By chelating the calcium ions with EDTA, the ions remain in solution but are inaccessible to the alginate chains and therefore unable to induce gelation upon mixture. By the addition of acetic acid to the continuous phase, the dissociation of the complex and release of calcium ions is triggered after drop formation. The free ions react with the alginate chains in a highly controlled fashion forming alginate microgels with excellent structural homogeneity. [74]

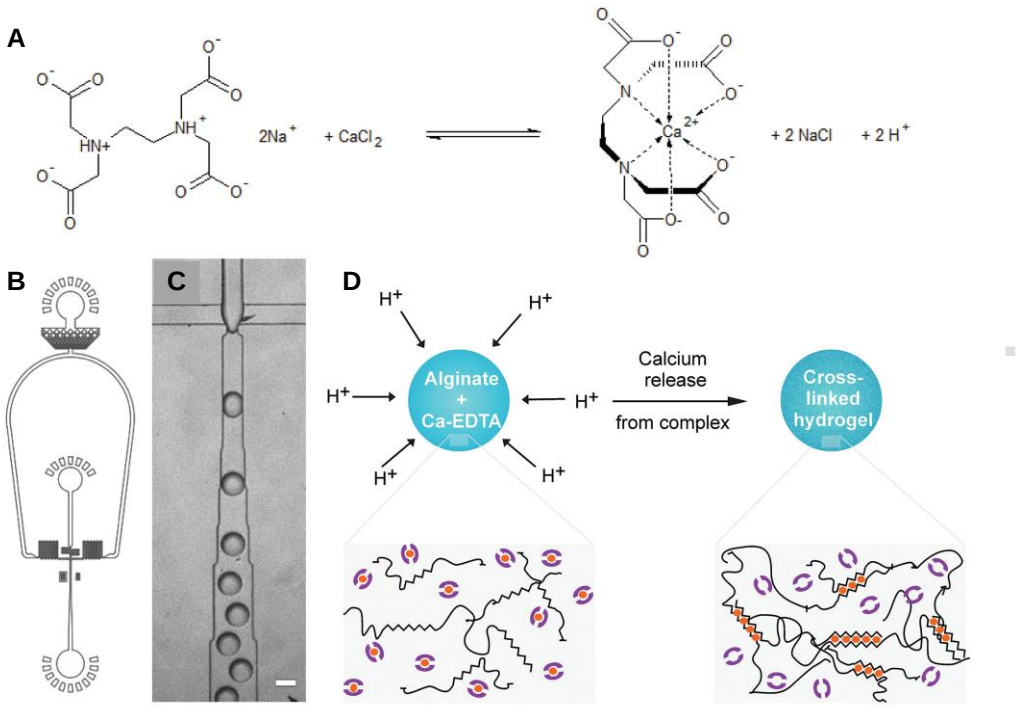

Figure 3-5 Microfluidic generation of monodispersed alginate microparticles by controlled release of calcium ions from the water-soluble calcium–EDTA complex. A) mechanism for gelation B, C) Schematic illustration of B) Microscopic image and C) The flow-focusing device used for the fabrication of alginate microbeads D) Schematic illustration of the crosslinking process. As the calcium–EDTA complex dissolves, calcium ions are released and crosslink the alginate. [74]

3.3.2 External gelation

In external gelation, cross-linkers are mixed with the particle after the alginate droplets form and are diffused into the alginate droplets or the microparticles formed. Unlike internal gelation, in which cross-linkers are always introduced directly in the microfluidic device, in external gelation, cross-linkers can be introduced both inside or outside of the device.

As Zhang et al. did, the cross-linkers were contained in the continuous fluid. Ca $(CH_3COO)_2$ was dissolved in soybean oil, the continuous fluid. Sodium alginate droplets were generated by a flow-focusing device in oil/Ca $(CH_3COO)_2$, with Spa80 as surfactant. Ca $(CH_3COO)_2$ diffused and dissolved in sodium alginate droplets along the channel and caused

external gelation on-chip. Finally, Ca-alginate hydrogel microparticles were collected in the oil. [75]

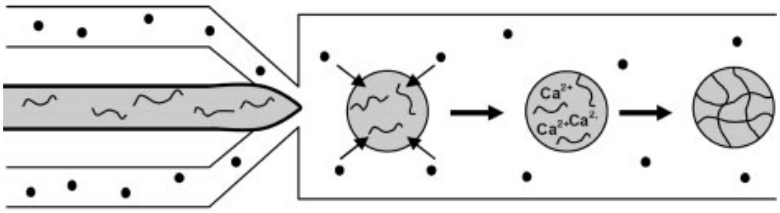

Figure 3-6 Schematic illustration of external gelation of alginate. Microparticles formed at the outlet were then mixed with crosslinker for gelation. [75]

And similar to internal gelation, clogging can be reduced by slowing down the diffusion of cross-linkers into alginate droplets. As demonstrated by Liu et al. they used emulsion fluids to introduce cross-linkers, using a glass microfluidic device with a modified hydrophobic channel.[76]. Droplets of sodium alginate were generated in corn oil at the first flow-focusing channel. The emulsion of $CaCl_2$, containing $CaCl_2$ droplets in corn oil, was injected downstream of the cross-junction. The contact between $CaCl_2$ and Na-alginate droplets caused ionic crosslinking and gelation of particles.

Chapter 4 Cell response to different substrate properties

4.1 Effect of substrate stiffness on cell behavior

It has been recognized that ECM proteins such as collagens, glycosaminoglycans, and proteoglycans can provide instructive messages to cells by transmitting the signal across the cell membrane through the transmembrane receptors that recognize these ECM proteins. These cell-ECM interactions influence cell behavior either directly or through combination with growth factors.[77] Furthermore, stem cells have been shown to respond to external mechanical loading.[78] Depending on these early studies, people started to realize that stiffness of the ECM is also a highly potent regulator of cell behavior.

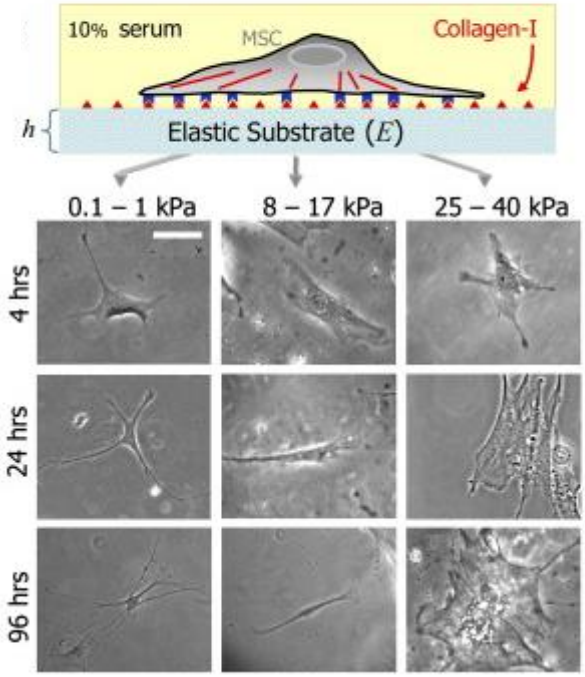

Figure 4-1 Stem cells grown on substrate with different show different morphologies and were prone to different lineage. [79]

Starting in the late 1990s, one study that used polyacrylamide hydrogels of varying

elastic moduli coated with ECM proteins as cell culture substrates showed that substrate stiffness affected cell-ECM adhesion, spreading, and migration.[80] Since this study, numerous groups have used polyacrylamide gels, and a variety of other material systems with tunable elastic moduli, to show that substrate stiffness impacts various other processes, including proliferation and apoptosis, stem cell differentiation, breast cancer progression and response to drugs[81, 82] Cells receive mechanical feedback from the substrate to which they adhere, even when there are no externally applied forces. In recent years, researchers have been extensively investigating the role of the stiffness of a substrate as one of the key parameters that affect cell behavior. A key motivation for this kind of study was that cells in vivo often are grown in a relatively soft environment, while conventional tissue culture flasks are very rigid. This diversity led to the development of 2D in vitro model systems, which use polymer gel substrates with tunable mechanical properties that are coated with specific ECM proteins for cell attachment. In particular, polyacrylamide gels have been widely used because these gels can be tuned within a wide range of stiffness that mimics those of natural tissues.[83-85] Commonly chosen stiffness values for the PA gels are in the range of ~0.5 kPa (brain tissue), ~10 kPa (muscle tissue), and >30 kPa (pre-mineralized bone). These gels are often referred to as ‘soft’, ‘intermediate stiff’, and ‘stiff’. [83] Various studies indicated that stiffer substrates generally promote cell spreading, whereas soft substrates induce a more rounded cell shape. [86, 87]And it is not surprising that those changes in cell morphology would also alter the cell behavior, including cell differentiation, as the organization of the cytoskeleton is reorganized. Mesenchymal stem cells were shown to specify lineage and commit to phenotypes with extreme sensitivity to substrate stiffness. Soft gels that mimic brain tissue

would induce neurogenesis of MSCs, while stiffer matrices that mimic muscle tissue induce myogenesis, and osteogenesis on rigid gels. At the start of the culturing, reprogramming of these lineages can still be performed with the addition of soluble induction factors, but after several weeks in culture, the cells commit to the lineage specified by matrix stiffness.[79]

4.2 Viscoelastic property of biological tissues

Typically, biomaterials used for cell experiments are linearly elastic substrates, often collagen- or fibronectin-coated polyacrylamide hydrogels. Linearly elastic materials behave like a spring, instantaneously deforming by an amount proportional to an applied load and returning to their original shape upon unloading. However, biological tissues behave like viscoelastic rather than linearly elastic materials. They exhibit a time-dependent mechanical response and dissipate a fraction of the energy it took to deform them, a property called viscoelasticity or poroelasticity, depending on the molecular mechanism.[88]

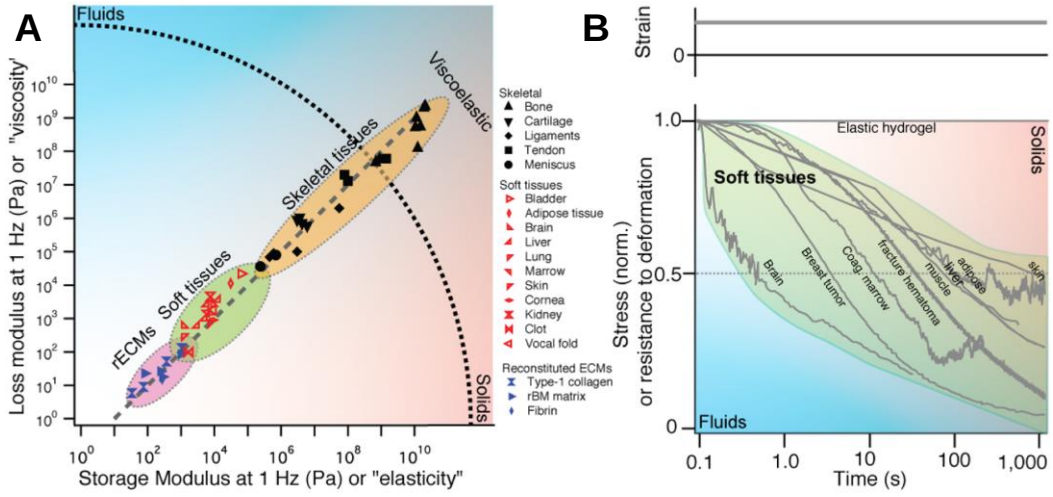

Figure 4-2 Viscoelasticity and stress relaxation of biological tissues and extracellular matrices A) Plot of loss modulus at ~1 Hz, a measure of viscosity (or dissipation), versus storage modulus at ~1 Hz, a measure of elasticity, for skeletal tissues, soft tissues, and reconstituted ECMs. B) Stress relaxation of different tissues. [88]

To be more specific, even when tissues globally recover shape after injury or disease,

local regions might not do so after forces are removed, experiencing irreversible or plastic deformations. Irreversible changes in cell-cell boundaries caused by cell-derived forces at junction sites have been found as essential features of pattern formation during the development of certain diseases like Drosophila.[89] As shown in figure 4.2, stress relaxation tests reveal that soft tissues, including the liver, breast, muscle, and skin could release the load applied on the tissue. This process of relaxing their resistance to deformation may take tens to hundreds of seconds.[88] Many soft tissues also exhibit nonlinear elasticity by strain-stiffening or become increasingly difficult to extend as they are deformed, which may be advantageous in preventing large deformations that damage tissue.[90] For example, in blood vessel walls, distensibility at low strains accommodates pulsatile blood flow while increased stiffness at high strains provides elastic stability to prevent vessel rupture. [91]

4.3 Effect of material viscoelasticity on cell behavior

The impact of substrate viscoelasticity on cells has been demonstrated powerfully through a set of 2D culture studies. In an early study, spreading for cells cultured on soft substrates that exhibit stress relaxation has been found to be greater than cells spreading on elastic substrates of the same modulus. 92 Another publication cultured human mesenchymal stem cells (hMSCs) on collagen-coated PA gels that had similar storage moduli, but varying loss moduli and creep responses.[92] Increased loss moduli or creep in the substrates promoted cell spreading, focal adhesion formation, cell proliferation, and differentiation towards adipocytes, osteoblasts, and smooth muscle cell lineages.

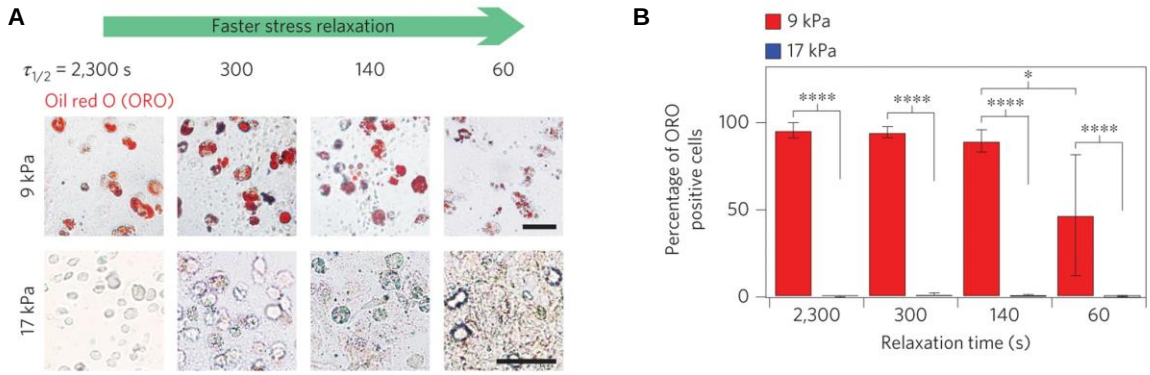

Figure 4-3 A) Images of cryosections with Oil Red O staining (red) that indicate adipogenic differentiation. MSC cultured in gels with low stiffness show adipogenic differentiation, while cells on substrate with faster stress relaxation show less tendency for adipogenic differentiation. B) Quantification of the percentage of cells staining positive for Oil Red O.[55]

Myosin and Rho-inhibition studies indicated the role of cytoskeletal tension in mediating the response to increased mechanical loss. In a follow-up study, increased activation of Rac1 and increases in motility and lamellipodial protrusions were found in hMSCs on substrates with higher loss and creep.[93] Another study compared fibroblasts and cancer cells cultured on covalently crosslinked(elastic), versus ionically crosslinked(viscoelastic) alginate gels that presented RGD cell adhesion ligands. These cells were unable to spread on soft elastic gels, but they could still spread on soft viscoelastic gels through β1 integrin, myosin, and Rho, while still exhibiting robust focal adhesions and stress fibers and upregulated YAP expression, similar to their behavior on stiff and elastic substrates[94]

Darnell et al. investigated how substrate stiffness, stress relaxation, and adhesion ligand density could affect the stem cell at the transcriptional level, using a 3D cell culture system that allows for the independent control of different mechanical cues.[95] As for mouse

mesenchymal stem cells and human cortical neuron progenitors, they found dramatic coupling among these substrate properties, and that the relative contribution of each property to changes in gene expression varies with cell type. In human neural progenitor cells(hNPCs), cells grown on the stress relaxation show a large amount of differentially expressed genes, which indicate a huge effect of substrate viscoelasticity on hNPCs.

4.4 Potential of using viscoelasticity to mediate T cell activation

It has been found that T cells can sense the mechanical properties of an activating substrate. O'Connor et al. demonstrated that mixed CD4+/CD8+ populations of primary human T cells activated on flat polydimethylsiloxane (PDMS) elastomer surfaces presenting anti-CD3 and anti-CD28 antibodies exhibit greater expansion on soft substrate (Young's modulus E ~100 kPa) compared to stiff (E ~2 MPa) surfaces.[96]

T cell proliferation and IL-2 secretion exhibited a biphasic response to substrate stiffness, which can be shifted by adjusting the density of activating antibodies. And not surprisingly, this mechanosensing property of T cells can be abrogated by inhibition of cellular contractility.[97] T cell morphology was modulated by stiffness at early time points. RNA-seq indicates that T cells show differing monotonic trends in upregulated genes and pathways towards both ends of the stiffness spectrum. These studies provide a framework of T cell mechanosensing and suggest an effect of ligand density that may reconcile different, contrasting patterns of stiffness sensing seen in previous studies.

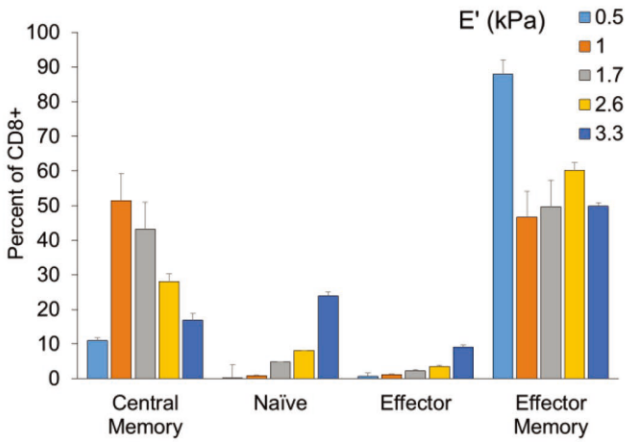

Figure 4-4 T cells stimulated on substrate with different stiffness show different phenotype, while one specific range of stiffness could promote the differentiation into memory T cells.[98]

It has also been found that substrate stiffness could change T cell phenotype. One study by Hicky et al. cultured T cells on antibody-conjugated hyaluronic acid (HA) hydrogel with different stiffness. They demonstrated that by changing the stiffness of the hydrogel, differences in phenotype, even within conditions that have similar fold expansions, can be observed. For example, the 0.5 and 1 kPa matrix both provided nearly 20-fold expansion, but the 1 kPa matrix generated a more balanced ratio of central memory to effector memory CD8+ T cells than the 0.5 kPa matrix. [98]

Chapter 5 Viscoelastic artificial aAPCs for T cell activation

5.1 Motivation

In cancer therapies, in particular, natural APCs activate and facilitate the expansion of tumor antigen-specific naive T cells which undergo further positive selection, differentiation, and maturation, inducing CD 8+ cytotoxic T cells that eventually kill the cancer cells. However, the therapeutic use of natural APCs has met limitations over the years as they lack the capacity for specific T cell-activating signals expression alteration.[99] To overcome this drawback, aAPCs have been developed to achieve both ex vivo and in vivo induction of antigen-specific cytotoxic T cells. A study has reported that artificial APCs retain the immunotherapeutic function while allowing for versatile properties control, including the size, shapes, and surface ligand density of the aAPCs.[99] The versatility of aAPCs is shown specifically in the commercialized Dynabeads, a type of polystyrene microbeads that can be conjugated with different antibodies for customized and accurate delivery of signals. The advantages of aAPCs have generated large interest in scientific research, leading to extensive studies showing that the T cell activation rate is affected by stiffness of the antigen-presenting surface. [94] A recent study revealed that alginate microgel with higher stiffness could improve cytokine production as well as T cell activation.[100] In another study, the spreading and expansion of cells could be modulated by stress relaxation of substrate, indicating the cell response to viscoelasticity of the extracellular matrix. [94] Chaudhuri et al. also underscored the significance of extracellular matrix viscoelasticity on cell signaling, transcription factor activation, and epigenome.[101] However, the effect that viscoelasticity of antigen-presenting

surface has on T cell activation is much less studied than that of the stiffness of aAPCs.

Based on the evidence of cell response to substrate viscoelasticity, as well as the mechanical sensing properties of t cells, a hypothesis can be made: T cells could sense the differences in viscoelasticity. Although T cell activation can be achieved by using antibody-coated plate, the adherent culture of T cells is not a natural process for T cell expansion, and could not replicate the formation of immune synapses during in vivo T cell activation. Therefore, a viscoelastic aAPCs system could serve as a perfect platform to study the T cell response to viscoelastic properties, compared to pure elastic matrices.

In this study, we aim to fabricate a type of viscoelastic aAPCs that can serve as a platform to study the effect of viscoelasticity on T cell activation. Cell-sized microparticles were fabricated using biocompatible alginate on a microfluidic platform. The hydrogel microbeads were then conjugated by T cell-specific antibodies (anti-CD3 & anti-CD28) to form artificial Antigen-Presenting Cells (aAPCs), which can be used for efficient in vitro T-cell activation. By tuning the molecular weight and cross-linker concentration, we can adjust the viscosity of aAPCs under consistent stiffness. In addition, by changing the cross-linking mechanism from ionic to covalent, purely elastic aAPCs without any viscoelastic properties will serve as a control group. Interleukin 2 (IL-2), a cytokine that is required for T cell expansion and activation, can be loaded into the aAPCs and achieve controlled release. This viscoelastic aAPCs can be used for studying the effect of viscoelastic properties on T cell activation, including T cell phenotype change, exhaustion, and expansion rate. It also possesses the potential to boost the therapeutic effectiveness of aAPCs in future clinical use.

5.2 Experimental design

5.2.1 Alginate microgel fabrication

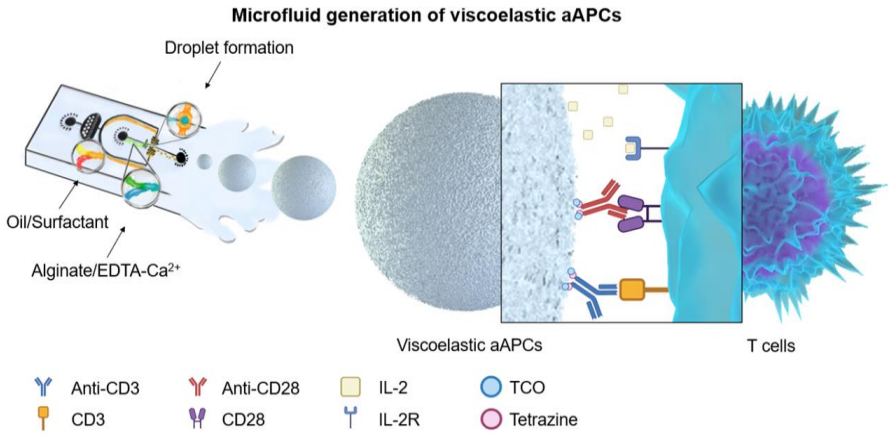

Figure 5-1 Scheme illustration of the microfluidic generation of viscoelastic artificial antigen-presenting cells (aAPCs) for T cell activation.

Fabrication of the viscoelastic aAPCs can be divided into two parts: alginate microgel generation and antibody conjugation to the alginate beads.

The gelation system consists of water phase and oil phase. The alginate is mixed with calcium–ethylenediaminetetraacetic acid (calcium–EDTA) in the water phase. Instead of mineral oil, Fluorinated carbon oil (HFE7500, 3 M) is used as the oil phase. This is a kind of engineering fluid with low viscosity and inert chemical properties, which helps stabilize the flow in the microfluidic device. By the addition of acetic acid to the oil phase, the dissociation of the complex and release of calcium ions is triggered after drop formation, while acetic acid dissolves into the water phase. The free ions react with the alginate chains in a highly controlled fashion forming alginate microgels.

Covalent beads serve as the control for viscoelastic beads, which can be fabricated by

transferring calcium-crosslinked beads to adipic acid dihydrazide(AAD) crosslinked covalent beads. Due to the slow gelation speed of AAD crosslinking(Minutes, compared to seconds for ionic crosslinking using Ca^{2+}), it is currently not feasible to produce monodispersed covalent alginate beads through a droplet-based microfluidic device directly, as the ungelled microbeads would immediately merge with each other and form clusters at the outlet of microfluidic devices.

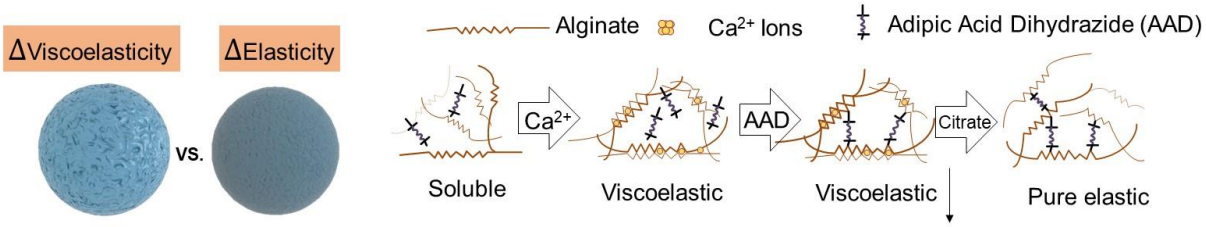

Figure 5-2 Schematic mechanism of converting viscoelastic alginate beads into covalent ones. A covalent crosslinker is added to the alginate microgel to form hybrid gel with both covalent and ionic crosslinking. Calcium in the gel is then removed by adding sodium citrate as chelator.

5.2.2 Evaluation of mechanical property

Mechanical properties of the aAPCs are tested using bulk gel with a similar composition to the microbeads. Fabrication of the bulk gel is based on published methods.[52]

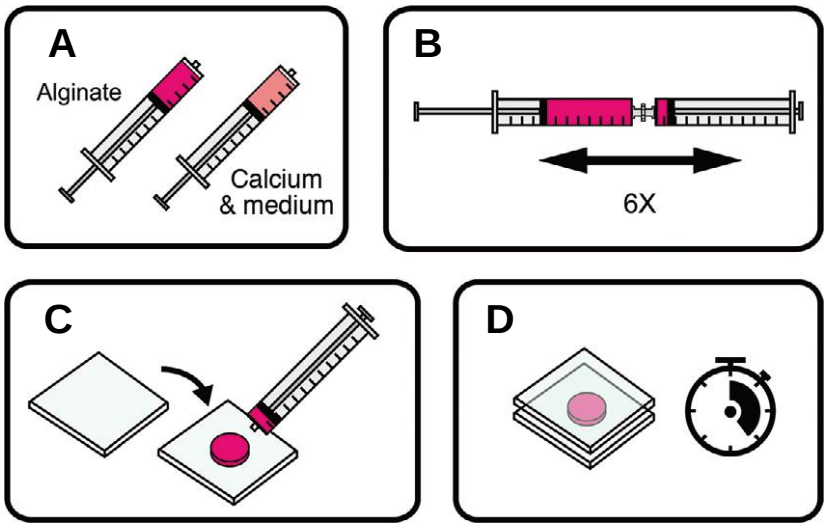

Figure 5-3 Overview of the basic steps for preparing alginate hydrogels. A) Loading alginate into the syringe. B)Alginate is rapidly mixed with calcium or covalent linker solution C) Blended solution is cast on glass slides D) 2h gelation for ionically crosslinked gel and overnight for covalently crosslinked gel.

The alginate beads are coated with anti-human CD3 antibody and anti-human CD8 antibody (Biolegend, USA) at 1:1 ratio using TCO-Tetrazine click chemistry. Trans–cyclooctene–tetrazine (TCO–Tetrazine) is the reaction pair that is suitable for biocompatible small molecule reactions commonly used in bioconjugation, allowing the joining of substrates of choice with specific biomolecules. This ligation chemistry is based on an inverse–demand Diels–Alder cycloaddition reaction between a trans–cyclooctene, and tetrazine reaction pair, forming a dihydropyridazine bond, shown in the figure above. The chemoselective TCO–Tetrazine ligation pair possess ultrafast kinetics (> 800 $M^{-1}s^{-1}$) and high reaction specificity.

5.2.3 Click chemistry conjugation

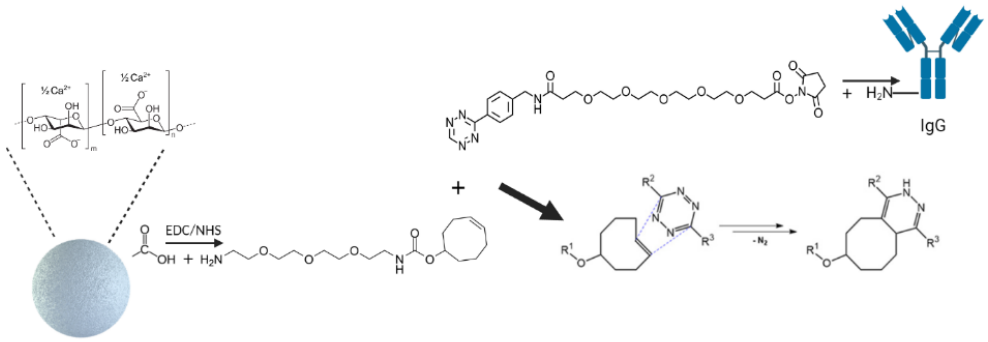

Figure 5-4 Basic concept of alginate-antibody conjugation through TCO-Tetrazine click chemistry.

To conjugate antibodies to alginate beads, TCO and Tetrazine are first conjugated to alginate beads and IgG antibody separately, using carbodiimide crosslinker chemistry, a reaction that crosslinks carboxylic acids to primary amines. Basically, 1-ethyl-(dimethylaminopropyl) carbodiimide ((EDC, Sigma Aldrich, USA), a water-soluble

carbodiimide was used to form amide linkages between the amine group on antibodies and the carboxylic acid on the alginate polymer. The co-reactant N-hydroxy- succinimide (NHS, Sigma Aldrich, USA) is a good leaving group that can stabilize the reactive EDC-intermediate against hydrolysis. In this study, TCO-PEG6-Amine(AxisPharm) and Tetrazine-PEG5-NHS(Sigma Aldrich) are picked for coupling antibodies to alginate beads.

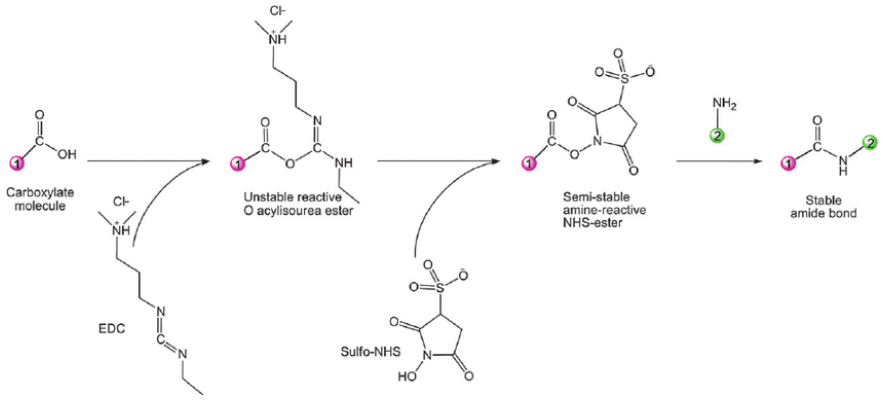

Figure 5-5 Schematic illustration of EDC/NHS coupling between carboxylic acids to primary amines. [102]

After conjugating the reaction pairs to alginate and antibody separately, these two reagents can be mixed and easily form a stable complex, which is the artificial antigen presenting cells we need for this study.

5.2.4 IL-2 loading & T cell activation

Due to the ability of alginate to encapsulate cytokines, IL-2, a cytokine that is important for T cell activation, can be also loaded into the aAPCs to achieve local delivery of co-stimulatory signal. The effect of viscoelastic aAPCs on T cell activation is evaluated by using the NFAT Reporter Jurkat T cells (ATCC, USA) that show upregulated firefly luciferase expression upon activation. Commercial aAPCs Dynabeads is used as the positive control

5.3 Methods

5.3.1 Microfluidic Device Fabrication:

All the photolithography works are conducted in the cleanroom at UCLA nanolab. The microfluidic patterns were etched on the 4-inch silicon wafers(Universitywafers, USA) using SU-8 photoresist. The microfluidic chip is molded from the silicone wafer using poly(dimethyl)siloxane (PDMS) (Sylgard 184 kit, Dow Corning). Channels were sealed by treating the PDMS mold and a glass microscope slide (VWR) with oxygen plasma. The channels are dried by air suction and kept in the oven at 65 °C until used.

5.3.2 Artificial APCs fabrication

The aAPCs are prepared by mixing the alginate solutions phase and oil phase in the phase formation microfluidic device. For the water phase, two kinds of alginate with different molecular weights (VLVG, MW:70 KD, and MVG, MW:280 KD, both from NovaMatrix) are mixed at a different ratio to adjust the viscoelasticity. For the oil phase, 157 FSH viscosity oil (Krytox) and acetic acid is added to the Novec 7500 engineering fluid. Both two solutions are injected into the microfluidic device from two different inlets, at a flow rate of 10:1 (oil phase/water phase). Alginate beads formed at the outlet are transferred into Novec 7500 containing 0.05% acetic acid. HEPES buffer containing 2mM calcium chloride (HEPES-Ca) is then added to the oil solution containing beads at 1:1 ratio, followed by a low speed centrifuge to separate two phases and transfer the beads from the oil phase to the water phase. The size distribution of the beads is obtained by imaging(At least 150 beads are counted)

5.3.3 Alginate beads-Antibody conjugation

(1) 3 million alginate beads are concentrated in MES buffer containing 2mM calcium chloride (MES-Ca) (pH=6.0). Both EDC/NHS are dissolved in MES-Ca buffer right before conjugation and mixed with beads. The reaction took 1h to attach NHS ester to the surface of alginate beads. After the reaction, the beads are washed with HEPES-Ca buffer containing 0.5% Tween20 (HEPES-Ca-Tween) to adjust the pH to 7. Then TCO-PEG6-Amine(USA) is added to the beads for overnight reaction to allow TCO conjugation onto the beads. The beads are then desalted by dialysis for 24h to remove excess TCO.

(2) Anti-CD3 and anti-CD28 antibody (Biolegend, San Diego, CA) are mixed at 1:1 ratio and concentrated in of PBS buffer using Amicon Ultra-2 spin column(Sigma Aldrich, USA), and mixed with Tetrazine-PEG5-NHS(Sigma Aldrich, USA) for 30 min reaction at room temperature. The antibody-tetrazine complex is then desalted using a spin column to remove excess Tetrazine. Purified Antibody-Tetrazine complex is mixed with glycerol at 1:1 ratio and preserved at -20 ℃.

(3)For TCO-Tetrazine click chemistry, the TCO-conjugated beads are concentrated in 100 ul HEPES-Ca buffer. 2 μg of antibody-tetrazine is then mixed with the beads and reacted for 2h at 37℃. The antibody- conjugated beads are washed three times with HEPES-Ca-Tween buffer and preserved at 4℃.

5.3.4 Covalent (elastic) beads fabrication

Alginate beads fabricated in 5.2.2 are incubated in MES-Ca buffer for 1h to adjust pH to 6 and mixed with EDC/NHS solution to activate the carboxylic acids on the surface of

alginate beads. PH is then adjusted to 7, followed by the addition of adipic acid dihydrazide (AAD) as covalent crosslinker. After overnight reaction, sodium citrate buffer is added to the beads to remove Ca^{2+} in the solution. The covalent beads are then washed with HEPES-Ca-Tween buffer and coated with T cell-specific antibody using the same method as viscoelastic beads, except that all the buffer used for conjugation does not contain Ca^{2+}.

5.3.5 IL-2 controlled release

The aAPCs fabricated from the process above were incubated in 10 ug/ml Il-2 solution for 12h. IL-2 release assays were conducted by incubating a suspension of 1 million aAPCs in 1 ml HEPES-Ca buffer. Every two days, particle suspensions were centrifuged and 100ul supernatant is collected as the sample. The same amount of HEPES-Ca-Tween buffer is added to the tube to keep the total volume. The amount of IL-2 in the supernatant was measured using a cytokine-specific ELISA kit (Biolegend, San Diego, CA)

5.3.6 Ligand density test

Quantification of the total amount of anti-CD3 and anti-CD28 presented on functionalized beads was analyzed using the micro-BCA assay kit (Thermo Fisher, USA) according to the manufacturer's protocol. After antibody conjugation, the supernatant was collected, and antibody concentration in the solution was measured by micro-BCA. The amount of antibody on each bead can be calculated, by dividing the total amount of antibody consumed in the reaction by the number of beads used for conjugation.

5.3.7 Bulk hydrogel preparation

For viscoelastic gel, alginate solution and calcium sulfide suspension are loaded into two syringes separately, at 4:1 ratio. Two syringes were then connected by a Luer lock connector, and the solution is rapidly mixed and immediately cast on the glass slide. After 2 h of crosslinking process, the hydrogel was cut into gel dishes with 8 mm diameter using a biopsy punch and incubated in HEPES-Ca buffer overnight.

For covalent gel, alginate is dissolved in MES buffer (pH=6) instead of water. Crosslinking solution containing EDC, hydroxybenzotriazole (HOBt), and different concentrations of AAD is prepared. Two solution is mixed and cast using a similar method to viscoelastic gel and allowed for overnight gelation.

Prepared hydrogel is then coated with anti-CD3 and anti-CD28 antibodies using similar protocol with beads. Briefly, each gel is immersed with MES buffer containing EDC and NHS for 1h. The solution was then replaced by the HEPES-Ca buffer, followed by the addition of TCO-PEG6-Amine and overnight reaction. After washing away the unreacted TCO, each gel is incubated with HEPES-Ca buffer containing Tetrazine-conjugated antibody for 3h. The antibody-coated gel was then washed and preserved in HEPES-Ca buffer for cell culture.

5.3.8 Mechanical property test

The stiffness of the particles is measured using bulk gel that has the same composition as the alginate beads. Young's modulus of the alginate gels is characterized by a Chatillon TCD-225 system (Tangent Labs) using TLC series load cells (AMETEK Sensors, Test &

Calibration). The data are collected and processed by Python using a published formula.[55] The initial loaded detected was used to calculate the elastic modulus. The time for the initial stress of the material to be relaxed to half of the initial value during a stress relaxation test is considered the relaxation time($\tau_{1/2}$).

5.3.9 Degradation test

Viscoelastic aAPCs conjugated with FITC-labeled antibodies are transferred from HEPS-Ca buffer into RPMI 1640 media and incubated at 37℃ for 14 days. Fluorescent images of the aAPCs are taken at different time points, and the fluorescence intensity is obtained by a microplate reader at the same time.

5.3.10 Cytotoxicity test

Viscoelastic aAPCs were cocultured with the Jurkat T cells. Cell viability is measured by Live/Dead staining kit (Thermo Fisher, USA) and quantified by ImageJ at day 0, day 1, and day 3. T cell cocultured with commercial Dynabeads is used as positive control.

5.3.11 T cell activation.

Different type of beads is first washed and resuspended in T cell culture media(RPMI 1640 supplemented with 10% FBS, 1% penicillin/streptavidin,50 μm 2-mercaptoethanol,1ng/ml puromycin). 1×10^5 NFAT Reporter Jurkat cells were seeded in the 96-well plate, beads are then added to the cells at a 1:1 ratio. The culture media is then supplemented with 30 IU/ml recombinant IL-2 to promote T cell activation. Images are

taken at 0h, 6h, and 24h after coculture. The activation level is then evaluated by the fluorescent intensity of each sample, which can be obtained by a microplate reader. The result is further confirmed by flow cytometry analysis.

5.4 Results

5.4.1 Microfluidic device for microparticle generation

The microfluidic device is designed by AutoCAD, containing two inlets for the oil phase and water phase separately. A filter structure is placed after the first inlet to reduce the clogging of the channel. The tortuous structure before the cross-section is used to slow down and stabilize the flow. Microparticles can form at the cross-section in a dripping mode.

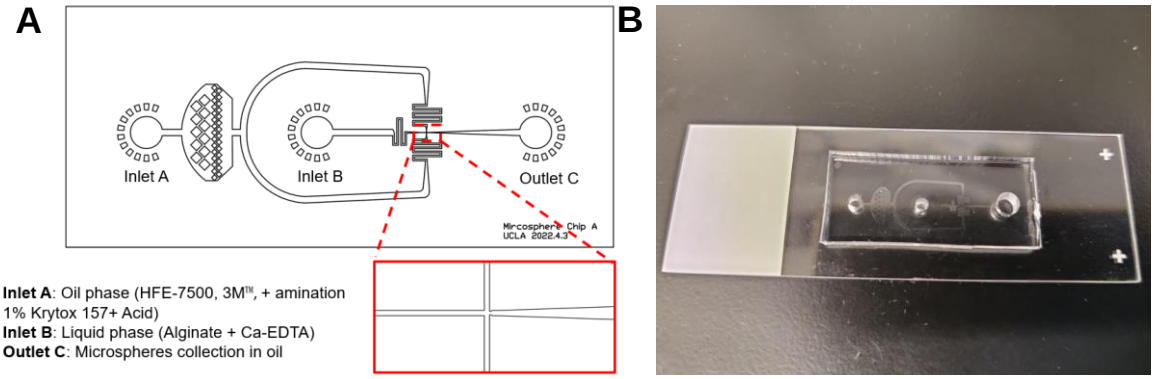

Figure 5-6 A) design of the droplet-based microfluidic device. B) Image of the PMDS microfluidic device.

Fabricated alginate beads have a homogeneous structure and good monodispersity. Viscoelastic beads and covalent beads did not show a significant difference in morphology, except that covalent beads are deeper in color, indicating that they may have higher density. As fig shows, by adjusting the flow rate, the size of beads can be slightly adjusted. The increased acetic acid concentration in the solution also speeds up the gelation process and

generates smaller beads. However, only some specific flow rate ratio of two inputs can achieve continuous production of microparticles. Other parameters may also cause imbalanced flow at the cross-section and impede the formation of beads.

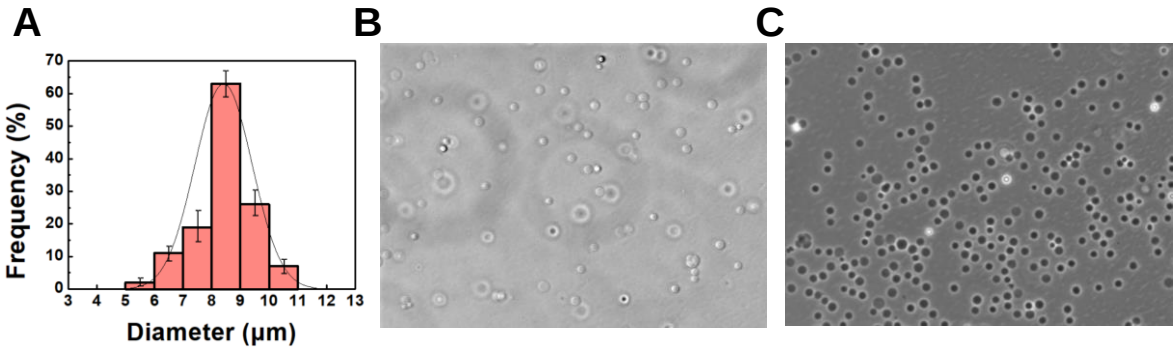

Figure 5-7 A) Size distribution histogram of homogeneous alginate beads. B) Representative image of viscoelastic beads. C) Representative image of elastic beads.

The fabricated alginate beads have a mean diameter of 8.41±0.99 μm, which shows the ability of this microfluidic device for continuous beads formation and stable size control.

The elastic beads have deeper color compared to viscoelastic one, probably due to the smaller mesh size and higher density. Generally, 10 million beads can be made per hour using this droplet-based microfluidic device, which indicates the potential of this design for high throughput alginate beads production.

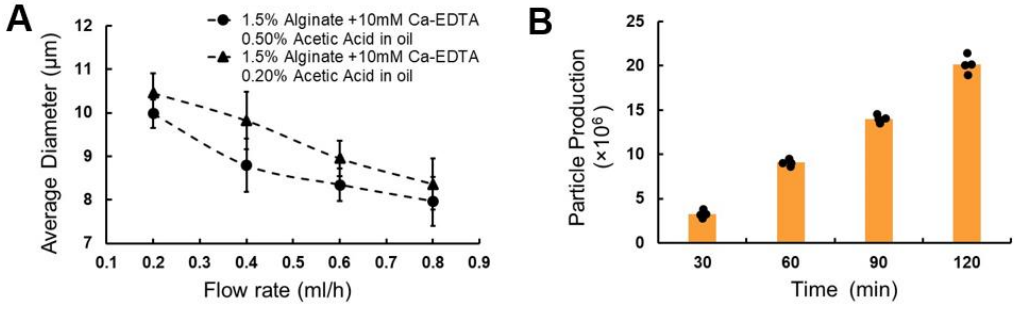

Figure 5-8 A) Average diameter of alginate beads based on flow rate and acetic acid concentration in the oil phase. B) Time course of beads production

Alginate beads coated with antibody form the complete aAPCs for cell study. It can be

observed that the alginate beads show even fluorescence on the surface, indicating that anti-CD3 & anti-CD28 are evenly distributed on the surface of the beads. Also, the low exposure time showed high fluorescence intensity on the surface, which equals to high surface ligand density. It has been argued that not all surface antibody conjugated on the microbeads is effective, due to the uncontrollable antibody orientation. The Fab region that is required for T cell recognition may not face outward, which makes these antibodies useless for T cell activation, even though they are conjugated to the beads. But this can be overcome by increasing surface ligand density, as there would still be enough amount of reachable antibodies in the right direction.

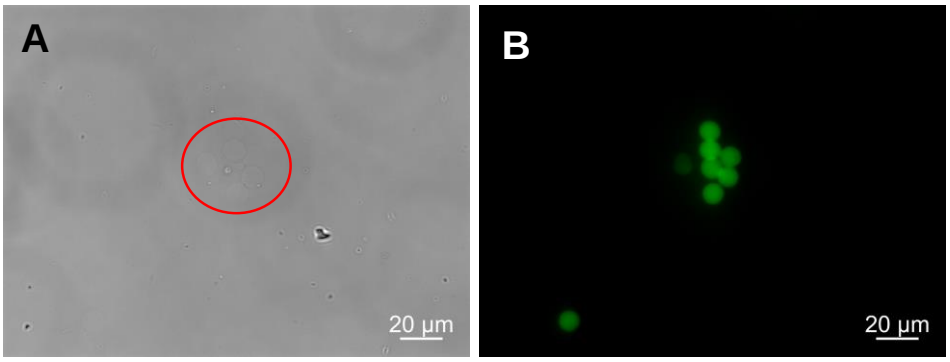

Figure 5-9 Image of artificial APCs conjugated with FITC-antibody. A) Bright field (particles highlighted in red circle) B) Fluorescence image, exposure time =300 ms.

Due to some difficulties in measuring the stiffness of alginate beads directly by atomic force microscopy, the mechanical properties of the alginate beads are measured by using bulk gel with the same composition as the beads instead.

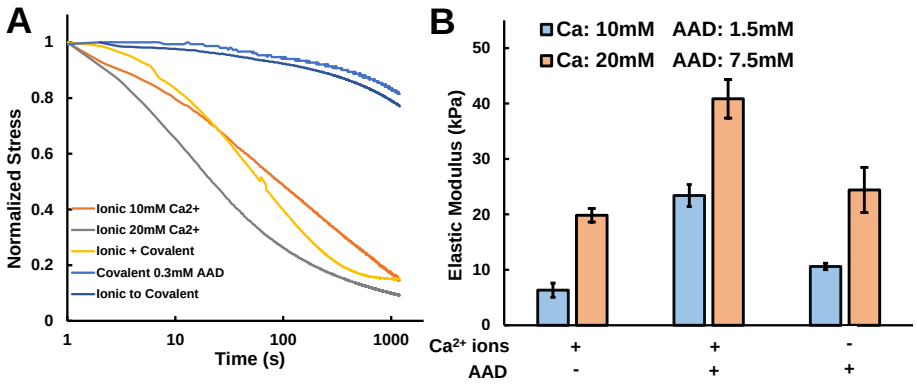

Figure 5-10 mechanical properties of viscoelastic, pure covalent, and converted covalent hydrogel.
A) Relaxation time B) Stiffness of viscoelastic and elastic hydrogel with different crosslinker concentrations.

As shown in figure 5.10 A), the Ionic crosslinked gel shows a relatively short relaxation time (42s for 10mM Ca^{2+} crosslinker, and 76s for 20mM Ca^{2+}) that is close to body tissue. While gel fabricated using higher crosslinker concentration have a higher degree of crosslinking and hence less stress relaxation. Although covalent gel does not have stress relaxation properties, slight stress relaxation can still be observed. This is caused by the incomplete gelation by using a low concentration of AAD crosslinker, and therefore those parts that are not crosslinked in the gel can still slide and dissipate part of the load applied to it.

As can be seen, the covalent gel transferred from viscoelastic gel shows a very similar relaxation time to pure elastic gel, which means the covalent aAPCs should also be pure elastic beads instead of the composite of ionic and covalent gel. And by adjusting the concentration of the crosslinker, the transferred covalent gel can have a similar stiffness to the viscoelastic gel 4.6 B). This proves that we can fabricate transferred covalent aAPCs with similar stiffness to the viscoelastic aAPCs.

5.4.2 IL-2 controlled release

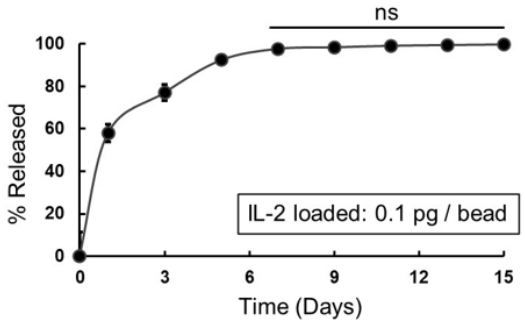

Figure 5-11 Time course of IL-2 sustained release

Due to the porosity of alginate microbeads, interleukin 2 can be retained in the beads and slowly released into the media during cell culture. According to the release profile, we observed a high initial burst on day 1, and all the IL-2 was released on day 7. Although this is not a perfect linear release, the sustained release of soluble IL-2 would infiltrate T cells, similar to how these cues are presented to T cells by natural APCs.

5.4.3 Degradation of viscoelastic aAPCs in culture media

During the fabrication process, alginate beads are preserved in buffer with 2mM calcium ions which can help stabilize the alginate crosslinked microgel. While the RPMI-1640 media contain only 0.6mM of Ca^{2+} and other phosphates that could affect the stability of the alginate beads, the degradation test is a must before coculture with cells

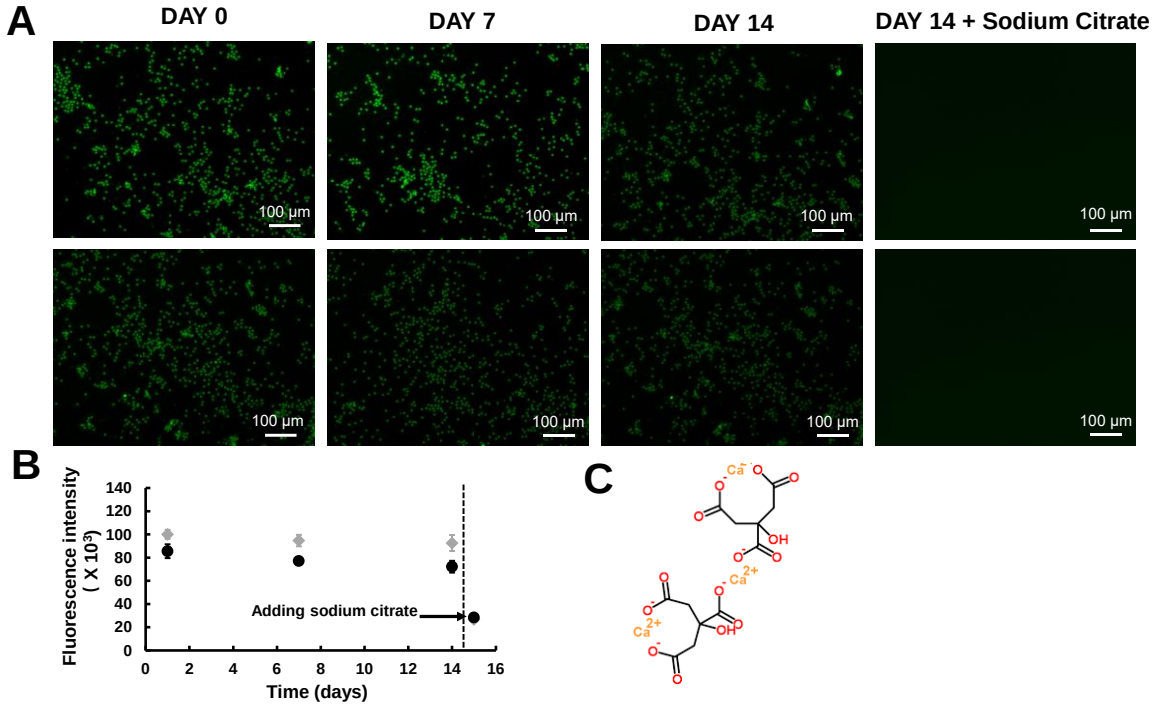

Figure 5-12 A) Degradation of viscoelastic aAPCs in RPMI-1640 culture media. Fluorescence intensity disappeared after the addition of sodium citrate buffer. B) Quantitative measurement of fluorescence using plate reader C) Mechanism for calcium chelation by citrate.

Based on the degradation test, the viscoelastic aAPCs incubated in RPMI-1640 media do not show significant degradation except for slightly diminished fluorescence intensity. Cell isolation after coculture can be achieved by adding 0.55mM sodium citrate buffer. Sodium citrate can chelate the calcium ions in solution, and the aAPCs were completely dissolved after calcium removal.

5.4.4 Ligand spacing

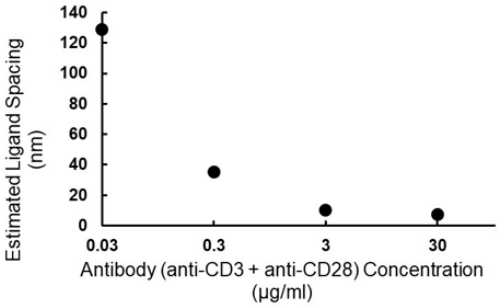

Figure 5-13 Ligand spacing for anti-CD3 & anti-CD28 on microbeads

Using the micro-BCA result, the average amount of antibody per unit on the beads can be calculated, and hence the ligand spacing. By varying the amount of antibody used in the conjugation, the ligand density on the microbeads can be adjusted. This can be used to investigate which ligand density gives the optimal T cell activation, since ultra-high ligand density may cause T cell exhaustion, while low ligand density would not be able to activate T cells. [103]

5.4.5 Cell viability

During the antibody coating of alginate beads, Tween20 is used to reduce shear stress so that the beads can be centrifuged down without being torn apart by the flow. Sodium is also added to the beads after conjugation to keep the aAPCs sterile. However, both agent is toxic to cells, which makes the cell viability test a must before T cell activation.

As the result in figure 5.10 shows, after 1 day of coculture with cells, the viscoelastic APCs group showed similar cell viability, compared to the control and commercial aAPCs Dynabeads.

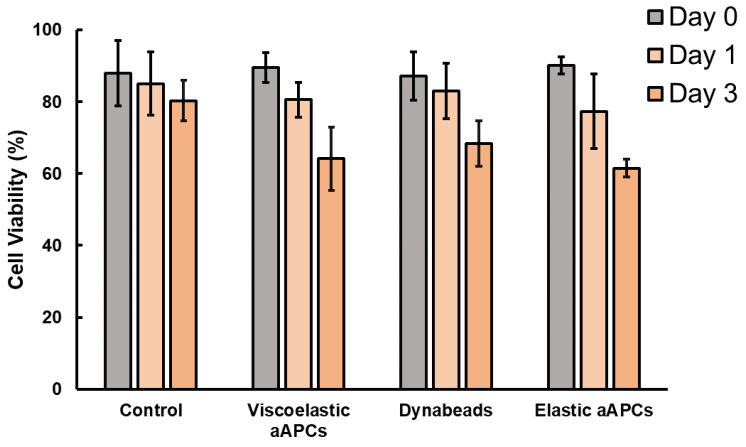

Figure 5-14 Cell viability after coculture with viscoelastic aAPCs and Dynabeads.

At day 3, the cell viability dropped to 66% and 64% for Dynabeads and viscoelastic APCs, relatively. This is probably caused by the activation-induced cell death (AICD), which happens during the in vitro activation using aAPCs.[104] But the viscoelastic APCs did not show significant cytotoxicity compared to the Dynabeads.

5.4.6 T cell activation test

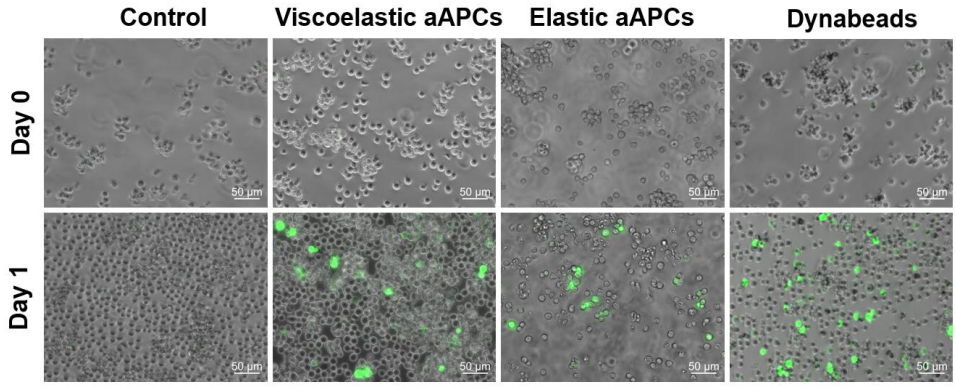

Figure 5-15 Images showing the activation of NFAT reporter T cells using Dynabeads and viscoelastic aAPCs.

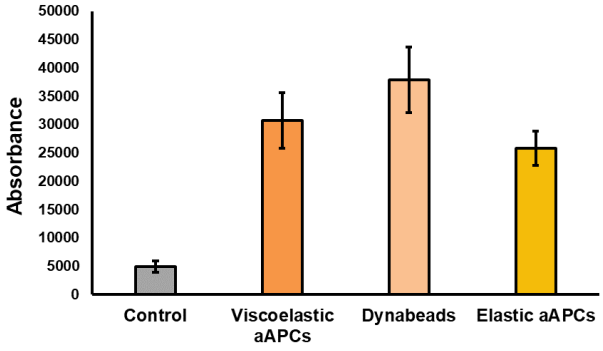

Figure 5-16 Fluorescence intensity measured by plate reader.

The activation is evaluated by using the fluorescence intensity of each well. As measured by the fluorescence intensity, viscoelastic aAPCs can activate a similar ratio of Jurkat Cells compared with Dynabeads, while the elastic one show slightly decreased activation. The absorbance value of the control is not close to zero, because the reporter Jurkat cells still express a low amount of GFP without being activated. This result is also

confirmed by flow cytometry analysis.

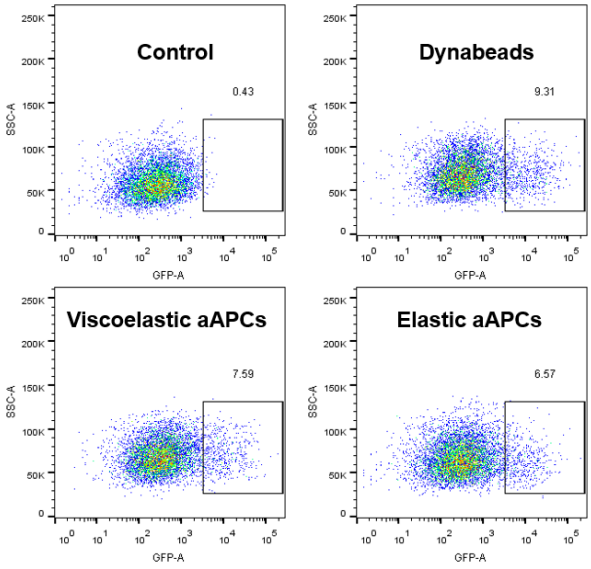

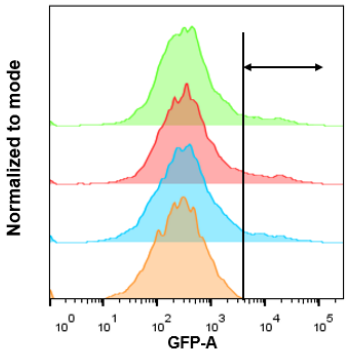

	Sample Name	Subset Name	Count
	Viscoelastic aAPCs	Single Cells	6359
	Dynabeads	Single Cells	6208
	Elastics aAPCs	Single Cells	6935
	Control	Single Cells	6556

Figure 5-17 FACS analysis of T cell activation.

The activated Jurkat cells were highlighted in the triangle in figure 5.11.2. After 24 h coculture, viscoelastic aAPCs are able to activate 7.6 % of the total cells, compared to 9.3% cells for Dynabeads. Elastic aAPCs also showed similar activation rate compared to viscoelastic ones. These results proved that the that both the viscoelastic aAPCs and elastic aAPCs have similar effects on T cell activation compared to the commercial Dynabeads, and have the potential for effective in vitro T cell expansion. Also, due to the difference in stress relaxation, this T cell stimulation platform can be used to study the effect of viscoelasticity on different T cell subtype, by varying the antibody conjugated on the beads.

Chapter 6 Conclusion and future works

The effect of substrate stiffness on cell behavior has been well studied, but how viscoelastic properties of biomaterials could affect cells, especially immune cells, has no conclusions so far. Therefore, a platform that could be used to study the effect of viscoelasticity on T cells could be very useful in demonstrating how T cells sense the mechanical properties of the substrate. Many studies on T cell mechanosensing have used antibody-coated 2D gel for cell culture, which is quite straightforward and cost-effective. But this is not a good mimic of the actual environment for T cell growth. By using viscoelastic aAPCs, T cells can be grown in suspension instead of seeding on the cells on the hydrogel. The deformable viscoelastic should be able to form a pretty tight immune synapse with T cells, which is required in vivo T cell activation.

Though there are many well-established methods for the generation of micrometer-sized alginate particles in pharmaceutical research, tissue engineering, and regenerative medicine, to our acknowledge, this is the first time that the alginate microgel particles (<10 μm) can be produced at high-throughput, with precise control over viscoelasticity properties and served as aAPCs to study the influence of the viscoelasticity on T cells activation. By changing the molecular weight of alginate and ligand density, different viscoelastic aAPCs can be customized for different T cell research.

However, although the aAPCs show good monodispersity and even antibody distribution on the surface, there is still some clustering during the fabrication process, which should be modified if the aAPCs are produced in larger quantities. Due to the time limit, the T cell fold

expansion study using primary mice T cells, which is a better estimate of T cell activation has not been included in this study. Also, the viscoelastic aAPCs are expected to generate less exhausted T cells, as they may generate CD3-TCR ligation and reduce repeated antibody stimulation. Further study including RNA sequencing can be performed between activated T cells using viscoelastic aAPCs & pure elastic aAPCs to figure out what genes play important roles in T cell sensing of the viscoelasticity.

As the mechanical properties of the viscoelastic aAPCs are closer to body tissues compared to the commercially used Polystyrene aAPCs, it may create a better environment for T cell activation compared to rigid and pure elastic aAPCs. Therefore, these viscoelastic aAPCs have such potential to improve the quality of in vitro expanded T cells and enhance the therapeutic effect of CAR T cells.

References

1. Almåsbak, H.; Aarvak, T.; Vemuri, M. C., Car T Cell Therapy: A Game Changer in Cancer Treatment. J Immunol Res **2016,** 2016, 5474602.

2. Sommermeyer, D.; Hudecek, M.; Kosasih, P. L., et al., Chimeric Antigen Receptor-Modified T Cells Derived from Defined Cd8+ and Cd4+ Subsets Confer Superior Antitumor Reactivity in Vivo. Leukemia **2016,** 30 (2), 492-500.

3. Salmon, H.; Franciszkiewicz, K.; Damotte, D., et al., Matrix Architecture Defines the Preferential Localization and Migration of T Cells into the Stroma of Human Lung Tumors. The Journal of Clinical Investigation **2012,** 122 (3), 899-910.

4. Maus, M. V.; Fraietta, J. A.; Levine, B. L., et al., Adoptive Immunotherapy for Cancer or Viruses. Annual Review of Immunology **2014,** 32 (1), 189-225.

5. Zhang, D. K. Y.; Cheung, A. S.; Mooney, D. J., Activation and Expansion of Human T Cells Using Artificial Antigen-Presenting Cell Scaffolds. Nature Protocols **2020,** 15 (3), 773-798.

6. Mizukami, A.; Swiech, K., Platforms for Clinical-Grade Car-T Cell Expansion. Methods Mol Biol **2020,** 2086, 139-150.

7. Kaiser, A. D.; Assenmacher, M.; Schröder, B., et al., Towards a Commercial Process for the Manufacture of Genetically Modified T Cells for Therapy. Cancer Gene Therapy **2015,** 22 (2), 72-78.

8. Vormittag, P.; Gunn, R.; Ghorashian, S., et al., A Guide to Manufacturing Car T Cell Therapies. Current Opinion in Biotechnology **2018,** 53, 164-181.

9. Dai, H.; Wang, Y.; Lu, X., et al., Chimeric Antigen Receptors Modified T-Cells for Cancer Therapy. JNCI: Journal of the National Cancer Institute **2016,** 108 (7).

10. Levine, B. L., Performance-Enhancing Drugs: Design and Production of Redirected Chimeric Antigen Receptor (Car) T Cells. Cancer Gene Therapy **2015,** 22 (2), 79-84.

11. Nguyen, L. T.; Yen, P. H.; Nie, J., et al., Expansion and Characterization of Human Melanoma Tumor-Infiltrating Lymphocytes (Tils). PLOS ONE **2010,** 5 (11), e13940.

12. Wherry, E. J., T Cell Exhaustion. Nature Immunology **2011,** 12 (6), 492-499.

13. Turtle, C. J.; Riddell, S. R., Artificial Antigen-Presenting Cells for Use in Adoptive Immunotherapy. Cancer J **2010,** 16 (4), 374-81.

14. Curtsinger, J.; Deeths, M. J.; Pease, P., et al., Artificial Cell Surface Constructs for Studying Receptor-Ligand Contributions to Lymphocyte Activation. J Immunol Methods **1997,** 209 (1), 47-57.

15. Neal, L. R.; Bailey, S. R.; Wyatt, M. M., et al., The Basics of Artificial Antigen Presenting Cells in T Cell-Based Cancer Immunotherapies. J Immunol Res Ther **2017,** 2 (1), 68-79.

16. Paulos, C. M.; Suhoski, M. M.; Plesa, G., et al., Adoptive Immunotherapy: Good Habits Instilled at Youth Have Long-Term Benefits. Immunologic research **2008,** 42 (1), 182-196.

17. Kim, J. V.; Latouche, J.-B.; Rivière, I., et al., The Abcs of Artificial Antigen Presentation. Nature biotechnology **2004,** 22 (4), 403-410.

18. Butler, M. O.; Lee, J. S.; Ansén, S., et al., Long-Lived Antitumor Cd8+ Lymphocytes for Adoptive Therapy Generated Using an Artificial Antigen-Presenting Cell. Clin Cancer Res **2007,** 13 (6), 1857-67.

19. Hirano, N.; Butler, M. O.; Xia, Z., et al., Engagement of Cd83 Ligand Induces Prolonged Expansion of Cd8+ T Cells and Preferential Enrichment for Antigen Specificity. Blood **2006,** 107 (4), 1528-36.

20. Zhang, H.; Snyder, K. M.; Suhoski, M. M., et al., 4-1bb Is Superior to Cd28 Costimulation for Generating Cd8+ Cytotoxic Lymphocytes for Adoptive Immunotherapy. The Journal of Immunology **2007,** 179 (7), 4910-4918.

21. Levine, B. L.; Bernstein, W. B.; Connors, M., et al., Effects of Cd28 Costimulation on Long-Term Proliferation of Cd4+ T Cells in the Absence of Exogenous Feeder Cells. The Journal of Immunology **1997,** 159 (12), 5921-5930.

22. Garlie, N. K.; LeFever, A. V.; Siebenlist, R. E., et al., T Cells Coactivated with Immobilized Anti-Cd3 and Anti-Cd28 as Potential Immunotherapy for Cancer. Journal of immunotherapy (Hagerstown, Md.: 1997) **1999,** 22 (4), 336-345.

23. Engelhard, V. H.; Strominger, J. L.; Mescher, M., et al., Induction of Secondary Cytotoxic T Lymphocytes by Purified Hla-a and Hla-B Antigens Reconstituted into Phospholipid Vesicles. Proc Natl Acad Sci U S A **1978,** 75 (11), 5688-91.

24. Wülfing, C.; Tskvitaria-Fuller, I.; Burroughs, N., et al., Interface Accumulation of Receptor/Ligand Couples in Lymphocyte Activation: Methods, Mechanisms, and Significance. Immunol Rev **2002,** 189, 64-83.

25. Zitvogel, L.; Regnault, A.; Lozier, A., et al., Eradication of Established Murine Tumors Using a Novel Cell-Free Vaccine: Dendritic Cell Derived Exosomes. Nature medicine **1998,** 4 (5), 594-600.

26. Wolfers, J.; Lozier, A.; Raposo, G., et al., Tumor-Derived Exosomes Are a Source of

Shared Tumor Rejection Antigens for Ctl Cross-Priming. Nature medicine **2001,** 7 (3), 297-303.

27. Olden, B. R.; Perez, C. R.; Wilson, A. L., et al., Cell-Templated Silica Microparticles with Supported Lipid Bilayers as Artificial Antigen-Presenting Cells for T Cell Activation. Advanced Healthcare Materials **2019,** 8 (2), 1801188.

28. Anel, A.; O'Rourke, A. M.; Kleinfeld, A. M., et al., T Cell Receptor and Cd8-Dependent Tyrosine Phosphorylation Events in Cytotoxic T Lymphocytes: Activation of P56lck by Cd8 Binding to Class I Protein. European journal of immunology **1996,** 26 (10), 2310-2319.

29. Oelke, M.; Maus, M. V.; Didiano, D., et al., Ex Vivo Induction and Expansion of Antigen-Specific Cytotoxic T Cells by Hla-Ig–Coated Artificial Antigen-Presenting Cells. Nature medicine **2003,** 9 (5), 619-625.

30. Laport, G. G.; Levine, B. L.; Stadtmauer, E. A., et al., Adoptive Transfer of Costimulated T Cells Induces Lymphocytosis in Patients with Relapsed/Refractory Non-Hodgkin Lymphoma Following Cd34+-Selected Hematopoietic Cell Transplantation. Blood **2003,** 102 (6), 2004-2013.

31. Rapoport, A.; Levine, B.; Badros, A., et al., Molecular Remission of Cml after Autotransplantation Followed by Adoptive Transfer of Costimulated Autologous T Cells. Bone marrow transplantation **2004,** 33 (1), 53-60.

32. Porter, D. L.; Levine, B. L.; Bunin, N., et al., A Phase 1 Trial of Donor Lymphocyte Infusions Expanded and Activated Ex Vivo Via Cd3/Cd28 Costimulation. Blood **2006,** 107 (4), 1325-1331.

33. Steenblock, E. R.; Wrzesinski, S. H.; Flavell, R. A., et al., Antigen Presentation on

Artificial Acellular Substrates: Modular Systems for Flexible, Adaptable Immunotherapy. Expert opinion on biological therapy **2009,** 9 (4), 451-464.

34. Gombotz, W. R.; Wee, S., Protein Release from Alginate Matrices. Advanced drug delivery reviews **1998,** 31 (3), 267-285.

35. Tønnesen, H. H.; Karlsen, J., Alginate in Drug Delivery Systems. Drug development and industrial pharmacy **2002,** 28 (6), 621-630.

36. Abasalizadeh, F.; Moghaddam, S. V.; Alizadeh, E., et al., Alginate-Based Hydrogels as Drug Delivery Vehicles in Cancer Treatment and Their Applications in Wound Dressing and 3d Bioprinting. Journal of Biological Engineering **2020,** 14 (1), 8.

37. Serunting, M. A.; Rusnadi, R.; Setyorini, D. A., et al., An Effective Cerium (Iii) Ions Removal Method Using Sodium Alginate-Coated Magnetite (Alg-Fe3o4) Nanoparticles. Journal of Water Supply: Research and Technology-Aqua **2018,** 67 (8), 754-765.

38. George, M.; Abraham, T. E., Polyionic Hydrocolloids for the Intestinal Delivery of Protein Drugs: Alginate and Chitosan—a Review. Journal of controlled release **2006,** 114 (1), 1-14.

39. Lee, K. Y.; Mooney, D. J., Alginate: Properties and Biomedical Applications. Progress in Polymer Science **2012,** 37 (1), 106-126.

40. Sakiyama-Elbert, S.; Hubbell, J., Functional Biomaterials: Design of Novel Biomaterials. Annual Review of Materials Research **2001,** 31, 183.

41. Varghese, S.; Elisseeff, J. H., Hydrogels for Musculoskeletal Tissue Engineering. Polymers for regenerative medicine **2006**, 95-144.

42. Grant, G. T., Biological Interactions between Polysaccharides and Divalent Cations: The

Egg-Box Model. Febs Lett. **1973,** 32, 195-198.

43. Mazumder, M. A. J., Bio-Encapsulation for the Immune-Protection of Therapeutic Cells. Advanced Materials Research **2013,** 810, 1-39.

44. Crow, B.; Nelson, K., Release of Bovine Serum Albumin from a Hydrogel-Cored Biodegradable Polymer Fiber. Biopolymers **2006,** 81 (6), 419-427.

45. Eiselt, P.; Lee, K. Y.; Mooney, D. J., Rigidity of Two-Component Hydrogels Prepared from Alginate and Poly (Ethylene Glycol)− Diamines. Macromolecules **1999,** 32 (17), 5561-5566.

46. Gattás-Asfura, K. M.; Stabler, C. L., Chemoselective Cross-Linking and Functionalization of Alginate Via Staudinger Ligation. Biomacromolecules **2009,** 10 (11), 3122-9.

47. Jeon, O.; Bouhadir, K. H.; Mansour, J. M., et al., Photocrosslinked Alginate Hydrogels with Tunable Biodegradation Rates and Mechanical Properties. Biomaterials **2009,** 30 (14), 2724-34.

48. Rowley, J. A.; Madlambayan, G.; Mooney, D. J., Alginate Hydrogels as Synthetic Extracellular Matrix Materials. Biomaterials **1999,** 20 (1), 45-53.

49. Zhao, X.; Huebsch, N.; Mooney, D. J., et al., Stress-Relaxation Behavior in Gels with Ionic and Covalent Crosslinks. J Appl Phys **2010,** 107 (6), 63509.

50. Grant, G. T.; Morris, E. R.; Rees, D. A., et al., Biological Interactions between Polysaccharides and Divalent Cations: The Egg-Box Model. FEBS Letters **1973,** 32 (1), 195-198.

51. Boontheekul, T.; Kong, H. J.; Mooney, D. J., Controlling Alginate Gel Degradation

Utilizing Partial Oxidation and Bimodal Molecular Weight Distribution. Biomaterials **2005,** 26 (15), 2455-65.

52. Charbonier, F.; Indana, D.; Chaudhuri, O., Tuning Viscoelasticity in Alginate Hydrogels for 3d Cell Culture Studies. Current Protocols **2021,** 1 (5), e124.

53. Graessley, W. W., Entangled Linear, Branched and Network Polymer Systems—Molecular Theories. In Synthesis and Degradation Rheology and Extrusion, Springer: 1982; pp 67-117.

54. Nam, S.; Stowers, R.; Lou, J., et al., Varying Peg Density to Control Stress Relaxation in Alginate-Peg Hydrogels for 3d Cell Culture Studies. Biomaterials **2019,** 200, 15-24.

55. Chaudhuri, O.; Gu, L.; Klumpers, D., et al., Hydrogels with Tunable Stress Relaxation Regulate Stem Cell Fate and Activity. Nature Materials **2016,** 15 (3), 326-334.

56. Song, H.; Tice, J. D.; Ismagilov, R. F., A Microfluidic System for Controlling Reaction Networks in Time. Angewandte Chemie International Edition **2003,** 42 (7), 768-772.

57. Hernández, R. M.; Orive, G.; Murua, A., et al., Microcapsules and Microcarriers for in Situ Cell Delivery. Advanced drug delivery reviews **2010,** 62 (7-8), 711-730.

58. Tran, V.-T.; Benoît, J.-P.; Venier-Julienne, M.-C., Why and How to Prepare Biodegradable, Monodispersed, Polymeric Microparticles in the Field of Pharmacy? International journal of pharmaceutics **2011,** 407 (1-2), 1-11.

59. Duncanson, W. J.; Lin, T.; Abate, A. R., et al., Microfluidic Synthesis of Advanced Microparticles for Encapsulation and Controlled Release. Lab on a Chip **2012,** 12 (12), 2135-2145.

60. Saralidze, K.; Koole, L. H.; Knetsch, M. L., Polymeric Microspheres for Medical

Applications. Materials **2010,** 3 (6), 3537-3564.

61. Seo, K.; Kim, D.; Sanchez, S., Fabrication and Applications of Complex-Shaped Microparticles Via Microfluidics. Lab on a Chip **2015,** 15 (18), 3622-3626.

62. Lee, T. Y.; Choi, T. M.; Shim, T. S., et al., Microfluidic Production of Multiple Emulsions and Functional Microcapsules. Lab on a Chip **2016,** 16 (18), 3415-3440.

63. Heida, T.; Neubauer, J. W.; Seuss, M., et al., Mechanically Defined Microgels by Droplet Microfluidics. Macromolecular Chemistry and Physics **2017,** 218 (2), 1600418.

64. Wang, W.; Zhang, M.-J.; Chu, L.-Y., Functional Polymeric Microparticles Engineered from Controllable Microfluidic Emulsions. Accounts of chemical research **2014,** 47 (2), 373-384.

65. Velasco, D.; Tumarkin, E.; Kumacheva, E., Microfluidic Encapsulation of Cells in Polymer Microgels. Small **2012,** 8 (11), 1633-1642.

66. Trantidou, T.; Friddin, M.; Elani, Y., et al., Engineering Compartmentalized Biomimetic Micro-and Nanocontainers. Acs Nano **2017,** 11 (7), 6549-6565.

67. Li, W.; Zhang, L.; Ge, X., et al., Microfluidic Fabrication of Microparticles for Biomedical Applications. Chem Soc Rev **2018,** 47 (15), 5646-5683.

68. Chu, L. Y.; Utada, A. S.; Shah, R. K., et al., Controllable Monodisperse Multiple Emulsions. Angewandte Chemie **2007,** 119 (47), 9128-9132.

69. Kim, S.-H.; Kim, J. W.; Cho, J.-C., et al., Double-Emulsion Drops with Ultra-Thin Shells for Capsule Templates. Lab on a Chip **2011,** 11 (18), 3162-3166.

70. Clausell-Tormos, J.; Lieber, D.; Baret, J.-C., et al., Droplet-Based Microfluidic Platforms for the Encapsulation and Screening of Mammalian Cells and Multicellular

Organisms. Chemistry & biology **2008,** 15 (5), 427-437.

71. Jeong, W. J.; Kim, J. Y.; Choo, J., et al., Continuous Fabrication of Biocatalyst Immobilized Microparticles Using Photopolymerization and Immiscible Liquids in Microfluidic Systems. Langmuir **2005,** 21 (9), 3738-3741.

72. Ochoa, A.; Trejo, F.; Olguín, L. F., Droplet-Based Microfluidics Methods for Detecting Enzyme Inhibitors. In Targeting Enzymes for Pharmaceutical Development: Methods and Protocols, Labrou, N. E., Ed. Springer US: New York, NY, 2020; pp 209-233.

73. Zhang, H.; Tumarkin, E.; Peerani, R., et al., Microfluidic Production of Biopolymer Microcapsules with Controlled Morphology. Journal of the american chemical society **2006,** 128 (37), 12205-12210.

74. Utech, S.; Prodanovic, R.; Mao, A. S., et al., Microfluidic Generation of Monodisperse, Structurally Homogeneous Alginate Microgels for Cell Encapsulation and 3d Cell Culture. Adv Healthc Mater **2015,** 4 (11), 1628-33.

75. Zhang, H.; Tumarkin, E.; Sullan, R. M. A., et al., Exploring Microfluidic Routes to Microgels of Biological Polymers. Macromolecular rapid communications **2007,** 28 (5), 527-538.

76. Liu, Y.; Tottori, N.; Nisisako, T., Microfluidic Synthesis of Highly Spherical Calcium Alginate Hydrogels Based on External Gelation Using an Emulsion Reactant. Sensors and Actuators B: Chemical **2019,** 283, 802-809.

77. Lin, C. Q.; Bissell, M. J., Multi-Faceted Regulation of Cell Differentiation by Extracellular Matrix. The FASEB Journal **1993,** 7 (9), 737-743.

78. Saha, S.; Ji, L.; de Pablo, J. J., et al., Inhibition of Human Embryonic Stem Cell

Differentiation by Mechanical Strain. J Cell Physiol **2006,** 206 (1), 126-37.

79. Engler, A. J.; Sen, S.; Sweeney, H. L., et al., Matrix Elasticity Directs Stem Cell Lineage Specification. Cell **2006,** 126 (4), 677-689.

80. Pelham, R. J., Jr.; Wang, Y., Cell Locomotion and Focal Adhesions Are Regulated by Substrate Flexibility. Proc Natl Acad Sci U S A **1997,** 94 (25), 13661-5.

81. DuFort, C. C.; Paszek, M. J.; Weaver, V. M., Balancing Forces: Architectural Control of Mechanotransduction. Nature reviews Molecular cell biology **2011,** 12 (5), 308-319.

82. Vogel, V.; Sheetz, M., Local Force and Geometry Sensing Regulate Cell Functions. Nature reviews Molecular cell biology **2006,** 7 (4), 265-275.

83. Rehfeldt, F.; Engler, A. J.; Eckhardt, A., et al., Cell Responses to the Mechanochemical Microenvironment—Implications for Regenerative Medicine and Drug Delivery. Advanced drug delivery reviews **2007,** 59 (13), 1329-1339.

84. Beningo, K. A.; Wang, Y.-L., Flexible Substrata for the Detection of Cellular Traction Forces. Trends in cell biology **2002,** 12 (2), 79-84.

85. Wong, J. Y.; Leach, J. B.; Brown, X. Q., Balance of Chemistry, Topography, and Mechanics at the Cell–Biomaterial Interface: Issues and Challenges for Assessing the Role of Substrate Mechanics on Cell Response. Surface science **2004,** 570 (1-2), 119-133.

86. Yeung, T.; Georges, P. C.; Flanagan, L. A., et al., Effects of Substrate Stiffness on Cell Morphology, Cytoskeletal Structure, and Adhesion. Cell motility and the cytoskeleton **2005,** 60 (1), 24-34.

87. Gaudet, C.; Marganski, W. A.; Kim, S., et al., Influence of Type I Collagen Surface Density on Fibroblast Spreading, Motility, and Contractility. Biophysical journal **2003,** 85 (5),

3329-3335.

88. Chaudhuri, O.; Cooper-White, J.; Janmey, P. A., et al., Effects of Extracellular Matrix Viscoelasticity on Cellular Behaviour. Nature **2020,** 584 (7822), 535-546.

89. Clément, R.; Dehapiot, B.; Collinet, C., et al., Viscoelastic Dissipation Stabilizes Cell Shape Changes During Tissue Morphogenesis. Current biology **2017,** 27 (20), 3132-3142. e4.

90. Storm, C.; Pastore, J. J.; MacKintosh, F. C., et al., Nonlinear Elasticity in Biological Gels. Nature **2005,** 435 (7039), 191-194.

91. Shadwick, R. E., Mechanical Design in Arteries. Journal of Experimental Biology **1999,** 202 (23), 3305-3313.

92. Cameron, A. R.; Frith, J. E.; Cooper-White, J. J., The Influence of Substrate Creep on Mesenchymal Stem Cell Behaviour and Phenotype. Biomaterials **2011,** 32 (26), 5979-5993.

93. Cameron, A. R.; Frith, J. E.; Gomez, G. A., et al., The Effect of Time-Dependent Deformation of Viscoelastic Hydrogels on Myogenic Induction and Rac1 Activity in Mesenchymal Stem Cells. Biomaterials **2014,** 35 (6), 1857-1868.

94. Chaudhuri, O.; Gu, L.; Darnell, M., et al., Substrate Stress Relaxation Regulates Cell Spreading. Nature communications **2015,** 6 (1), 1-7.

95. Darnell, M.; O'Neil, A.; Mao, A., et al., Material Microenvironmental Properties Couple to Induce Distinct Transcriptional Programs in Mammalian Stem Cells. Proceedings of the National Academy of Sciences **2018,** 115 (36), E8368-E8377.

96. Lambert, L. H.; Goebrecht, G. K.; De Leo, S. E., et al., Improving T Cell Expansion with a Soft Touch. Nano letters **2017,** 17 (2), 821-826.

97. Yuan, D. J.; Shi, L.; Kam, L. C., Biphasic Response of T Cell Activation to Substrate

Stiffness. Biomaterials **2021,** 273, 120797.

98. Hickey, J. W.; Dong, Y.; Chung, J. W., et al., Engineering an Artificial T-Cell Stimulating Matrix for Immunotherapy. Adv Mater **2019,** 31 (23), e1807359.

99. Vining, K. H.; Mooney, D. J., Mechanical Forces Direct Stem Cell Behaviour in Development and Regeneration. Nat Rev Mol Cell Biol **2017,** 18 (12), 728-742.

100. Tan, W.-H.; Takeuchi, S., Monodisperse Alginate Hydrogel Microbeads for Cell Encapsulation. Advanced Materials **2007,** 19 (18), 2696-2701.

101. Zhu, K.; Yu, Y.; Cheng, Y., et al., All-Aqueous-Phase Microfluidics for Cell Encapsulation. ACS Applied Materials & Interfaces **2019,** 11 (5), 4826-4832.

102. Bart, J.; Tiggelaar, R.; Yang, M., et al., Room-Temperature Intermediate Layer Bonding for Microfluidic Devices. Lab Chip **2009,** 9 (24), 3481-8.

103. Majzner, R. G.; Rietberg, S. P.; Sotillo, E., et al., Tuning the Antigen Density Requirement for Car T-Cell Activity. Cancer Discov **2020,** 10 (5), 702-723.

104. Appel, H.; Seth, N. P.; Gauthier, L., et al., Anergy Induction by Dimeric Tcr Ligands. The Journal of Immunology **2001,** 166 (8), 5279-5285.